MANCHESTER 1824

The University of Manchester

Plasma basics: instabilities, magnetic reconnection and particle acceleration

Philippa Browning
Jodrell Bank Centre for Astrophysics
University of Manchester

- Plasma instabilities and ideal MHD instabilities
- Resistive instabilities and “classical” reconnection models
- Some developments in reconnection modelling
  - Beyond MHD
  - 3D reconnection
- Reconnection in the corona and coronal heating
  - Relaxation and helicity
- Reconnection, solar flares and particle acceleration

The MHD equations

$$\frac{\partial \mathbf{B}}{\partial t} = \nabla \times (\mathbf{v} \times \mathbf{B}) + \eta \nabla^2 \mathbf{B}, \quad \eta = \frac{1}{\mu_0 \sigma},$$

$$\rho\left(\frac{\partial \mathbf{v}}{\partial t} + \mathbf{v}.\nabla \mathbf{v}\right) = -\nabla p + \mathbf{j} X \mathbf{B} + \rho \mathbf{g} + \mathbf{F},$$

$$\frac{\partial \rho}{\partial t} + \nabla.(\rho \mathbf{v}) = 0,$$

$$p = (k_B / m) T,$$

$$\frac{\rho^\gamma}{\gamma - 1}\left(\frac{\partial}{\partial t} + \mathbf{v}.\nabla\right)\left(\frac{p}{\rho^\gamma}\right) = -\nabla.(\kappa.\nabla T) - \rho^2 Q(T) + \frac{j^2}{\sigma} + H$$

MHD timescales

- Resistive (Ohmic) dissipation alone leads to a time-scale for resistive diffusion $t_D = L^2/\eta$
- The timescale for propagation of Alfven waves $v_A = \frac{B}{\sqrt{\mu_0 \rho}}$

  is $t_A = L/v_A$

This is the natural dynamic scale

- The ratio of the two timescales is the Lundquist number (S) – S is very large in solar atmosphere (hence resistive diffusion is very slow and ineffective!)

$$\boxed{\begin{array}{l} S = t_d / t_A = L v_A / \eta \\ \approx 10^{12} - 10^{13} \text{ in solar corona} \end{array}}$$

- "Ideal MHD" is limit of infinite S

Plasma instabilities and ideal MHD stability

Linear stability theory: normal modes

- Consider background static equilibrium ($\mathbf{B_0}$, p_0) with small fluid displacement ξ

$$\frac{\partial \xi}{\partial t} = \mathbf{v}_1$$

- Linearise momentum equation (small disturbances) and combine with induction equation:

$$\rho_0 \frac{\partial^2 \xi}{\partial t^2} = \mathbf{F}(\xi) \equiv \frac{1}{\mu_0}\left[(\nabla\times(\nabla\times(\xi\times\mathbf{B}_0)))\times\mathbf{B}_0 + (\nabla\times\mathbf{B_0})\times(\nabla\times(\xi\times\mathbf{B}_0))\right] + \nabla\left[\xi.\nabla p_0 + \gamma p_0(\nabla.\xi)\right]$$

- Assume all perturbed quantities have harmonic dependence $e^{i\omega t}$ where imaginary ω corresponds to instability (exponential growth)
- Find (real) eigenvalues ω^2 *of* $-\rho_0\omega^2\xi = \mathbf{F}(\xi)$
- Unstable if $\omega^2 < 0$

Linear stability theory: energy method

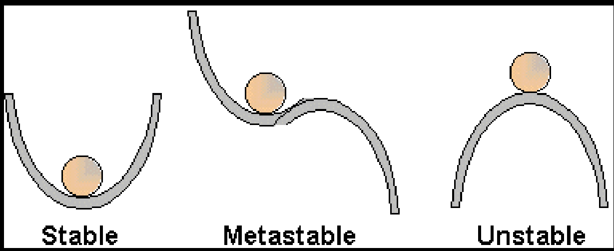

- Volume integral of equation of motion gives

δK + δW = constant

where perturbed kinetic energy and potential energy are

$$\delta K = \frac{1}{2}\int_V \rho_0 \left|\frac{\partial \xi}{\partial t}\right|^2 dV, \quad \delta W = -\frac{1}{2}\int_V \xi^* \cdot \mathbf{F}(\xi) dV$$

Hence it can be shown that field is **stable** if δW ≥ 0 for all possible displacements ξ

- Can demonstrate **instability** by using class of trial functions (obeying boundary conditions) and minimising δW – if δW can be negative for some ξ, field is unstable
- By manipulation of integral, perturbed potential energy can be written (in case of perfectly conducting walls) as

$$\delta W = \frac{1}{2}\int_V \left[\frac{1}{\mu_0}\left|\nabla\times(\xi\times\mathbf{B}_0)\right|^2 + \gamma p_0 |\nabla\cdot\xi|^2 - \xi^*.\mathbf{j}_0 \times \{\nabla\times(\xi\times\mathbf{B}_0)\} - \xi^*.\nabla(\xi.\nabla p_0)\right] dV$$

- First two terms (+) are stabilising
  - Field line bending (term 1) and compression (term 2)
- Second two terms (possibly -) can be destabilising due to sources of free energy
  - Equilibrium current (term 3) → kink instability
  - Pressure gradients (term 4) → ballooning/interchange instabilities

- **Gravity** and **equilibrium flows** (not included in above equation) can also drive instability

Example: Rayleigh Taylor Instability

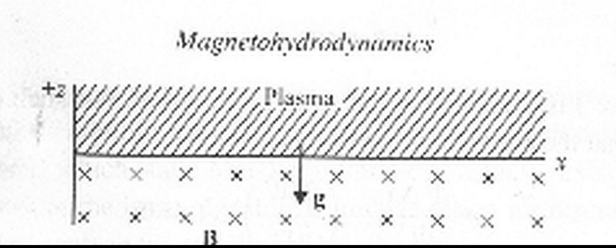

•Plasma suspended by horizontal magnetic field with gravity – magnetic pressure balances gravity

•Make small displacement or interchange

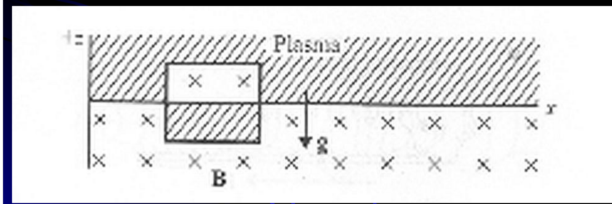

•Magnetic field energy unchanged, plasma potential energy decreases – hence unstable (perturbation will grow

$$\delta W = \delta \int_V \frac{B^2}{2\mu_0} \mathrm{d}V + \delta \int_V \rho g z \mathrm{d}V < 0$$

Rayleigh-Taylor instability

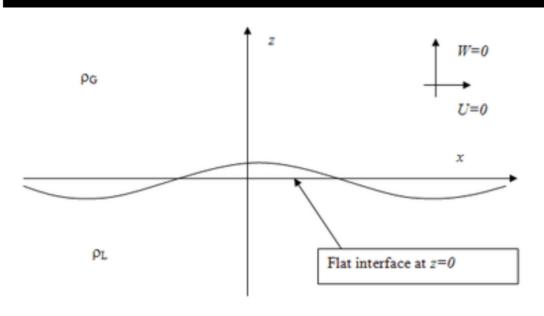

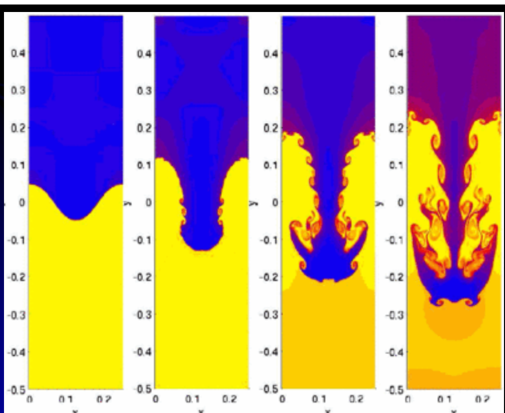

- Requires gravity (or accelerating reference frame)
- Heavy fluid suspended over light fluid is unstable – similarly stratified fluid is unstable if dρ/dz > 0
- Similar instability if fluid is supported against gravity by horizontal magnetic field (aka Kruskal-Schwartzschild instability/Parker instability/gravitational instability) – or accelerating transverse to interface

Buoyancy and Parker instability

- Magnetic buoyancy – consider an isothermal horizontal magnetic flux tube in local force balance with surroundings. Tube has lower thermal pressure due to magnetic pressure, hence it is lighter than surroundings

$$p_i + \frac{B^2}{2\mu_0} = p_e \Rightarrow \rho_i - \rho_e = -\frac{m_p B^2}{4\mu_0 kT}$$

- Upwards buoyancy force $(\rho_i - \rho_e)\, g$

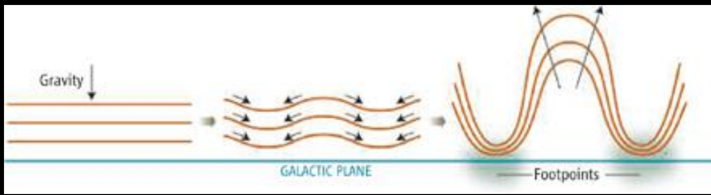

- Causes new magnetic flux to emerge at solar surface, sunspot formation – also important in galactic magnetic field
- Horizontal field is unstable to Parker instability when buoyancy overcomes magnetic tension, if *dB*/*dz* <0 – requires wavelength greater than critical wavelength $\lambda > 4\Lambda\left(1+\beta^{-1}\right)^{-1/2};\ \beta = 2\mu_0 p / B^2, \Lambda = kT/mg$

- Parker instability in solar convection zone
- Leads to flux emergence

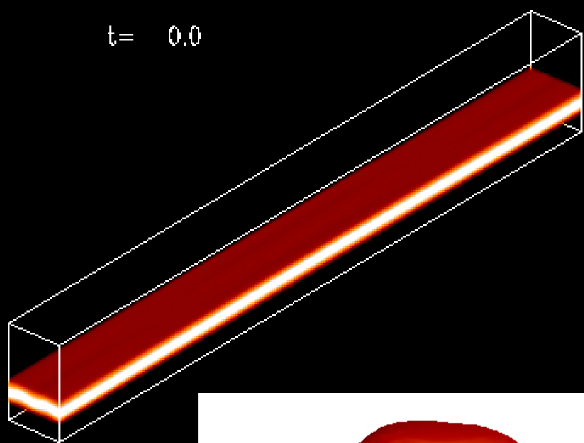

Fan Ap J 2001

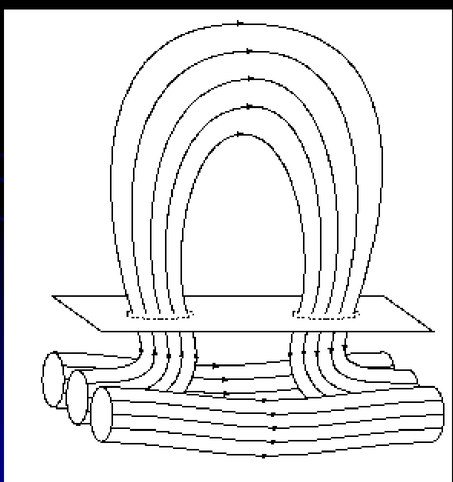

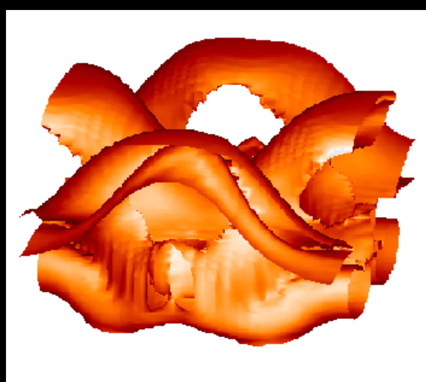

Matthews et al, 1995

Rayleigh-Taylor (Parker) instability in solar corona

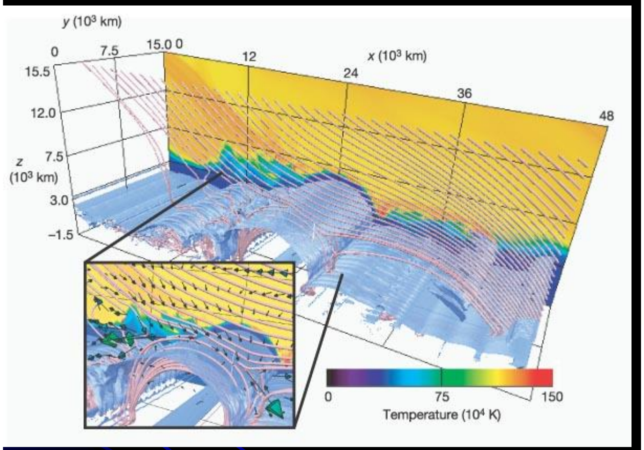

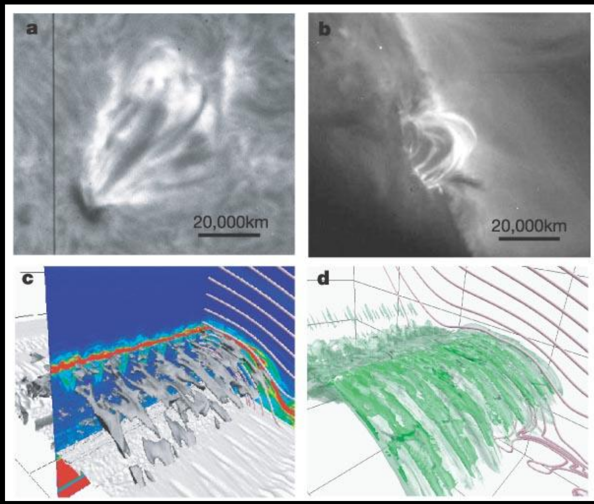

- Simulations and observations of emerging magnetic flux in solar corona *Isobe et al 2005*
- R-T instability creates filamentation – leads to reconnection and enhanced plasma heating

Rayleigh Taylor in solar prominences

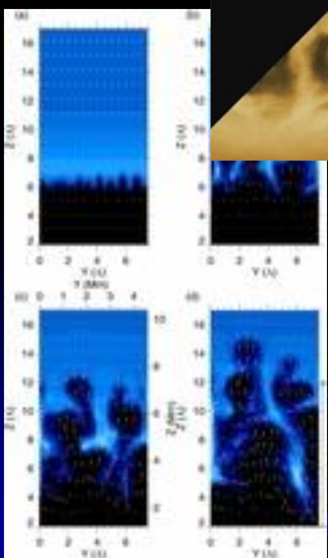

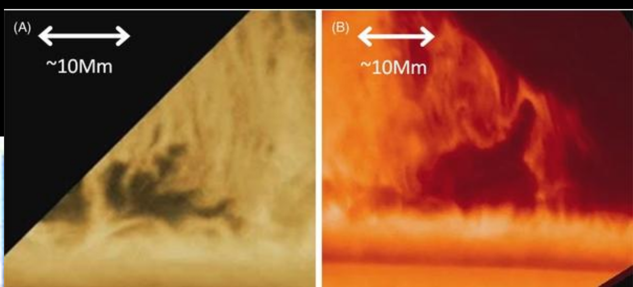

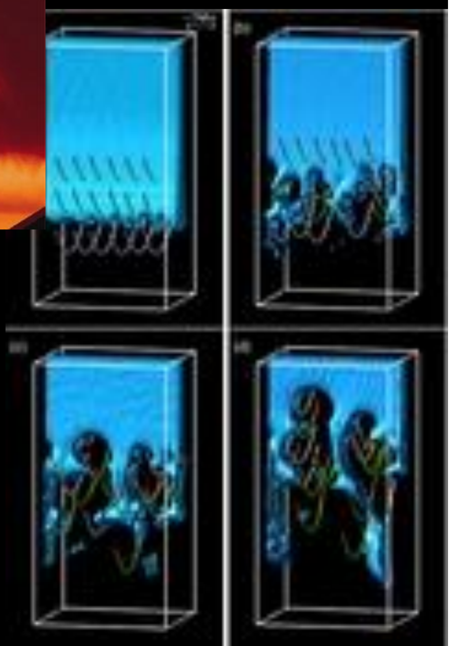

Dark upflows in prominences associated with RT instability
Hillier et al Ap J 2012

Rayleigh Taylor a "plasma" view –

e.g. plasma moving on curved field lines

- Simple model – cold plasma ($\beta = 0$), uniform B_0
- Ion flow – gravitational drift

$$\mathbf{v}_0 = \frac{m_i}{e}\frac{1}{B_0^2}\mathbf{g}\times\mathbf{B}_0 = -\frac{g}{\omega_c}\hat{\mathbf{y}}$$

- Linearise ion equation of motion - assuming

exp(i(ky-ωt)) dependence

$$m_i n_0(\omega - kv_0) = en_0(\mathbf{E}_1 + \mathbf{v}_1\times\mathbf{B}_0)$$

See Chen Chapter 6 for full details

Effective **g** due to centrifugal force

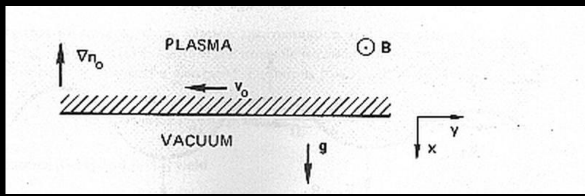

If a ripple develops, charge builds up on one side of ripple → electric field $\mathbf{E}_1$ → growth of ripple from $\mathbf{E}_1 \times \mathbf{B}_0$ drift

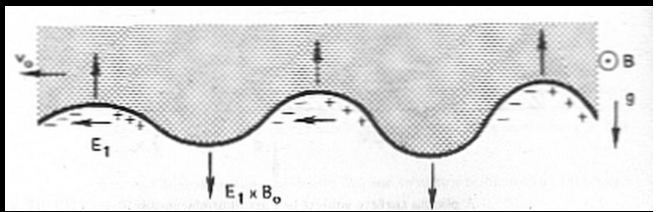

- Linearised continuity equation for ions

$$-i\omega n_1 + ikv_0 n_1 + v_{1x}n_0' + ikn_0 v_{1y} = 0$$

- Similarly for electrons (in limit of $m_e/m_i \to 0$)
- Combining gives

$$\omega^2 - kv_0\omega - g(n_0'/n_0) = 0$$
$$\Rightarrow \omega = \frac{1}{2}kv_0\left[\frac{1}{4}k^2v_0^2 + g\left(\frac{n_0'}{n_0}\right)\right]^{1/2}$$

- Hence instability (imaginary ω) requires $-g(n_0'/n_0) > \frac{1}{4}k^2v_0^2$

so density gradient must be in opposite direction to gravity

i.e. Heavy fluid suspended over light fluid or

Field line curvature bending away from plasma ("unfavourable curvature") are unstable

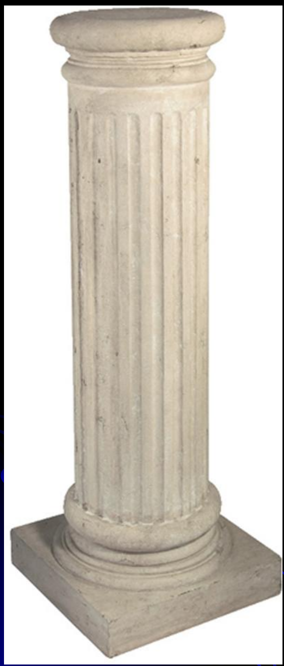

- Instability is stabilised by field line bending
- Hence perturbations have $\mathbf{k} \perp B_0$ constant along field lines
- Sometimes called "flute mode"
c.f. Fluted Greek column

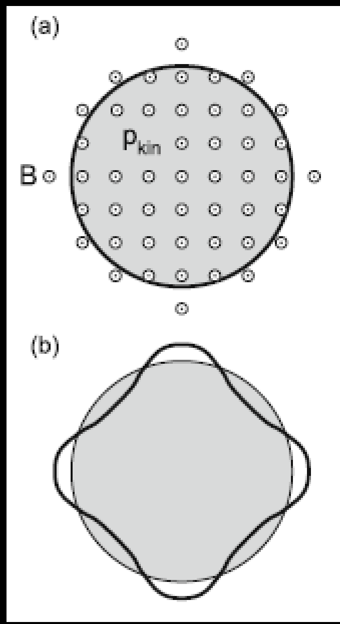

Sausage and kink instability

- An ideal MHD instability driven by **current** (twisted magnetic fields)
- **Kink** - increased magnetic pressure on "inside of bend" drives further displacment - creates helical distortion
- Stabilised by axial field (B_z) – field line bending (tension)
- Coronal loops with "line-tying" at dense photospheric footpoints are unstable if a critical twist ($\Phi = LB_\theta/rB_z$) is exceeded (*Hood and Priest 1979*)
- May create current sheets in nonlinear phase leading to reconnection and energy dissipation (see later)

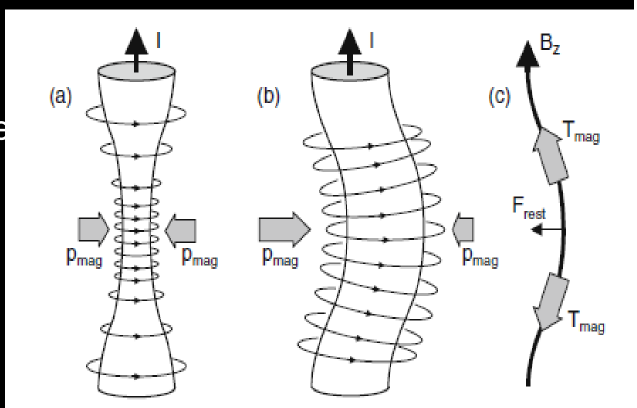

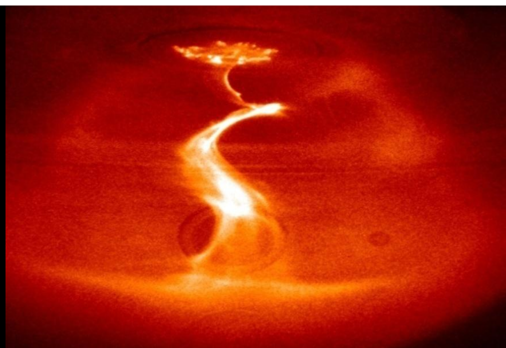

Hsu and Bellan 2002

Kink unstable toroidal flux rope in laboratory

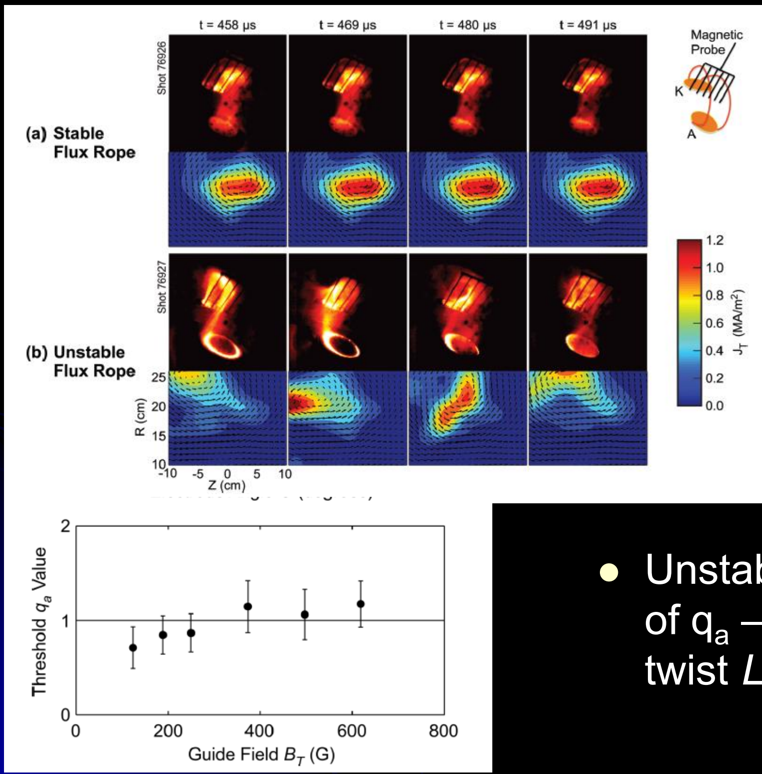

MRX experiment

Oz et al 2011

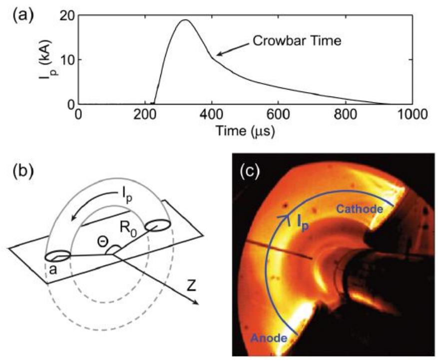

- Unstable for critical value of q_a – sufficiently strong twist LB_θ/rB_z

Rayleigh Taylor instability in kink unstable plasma loop

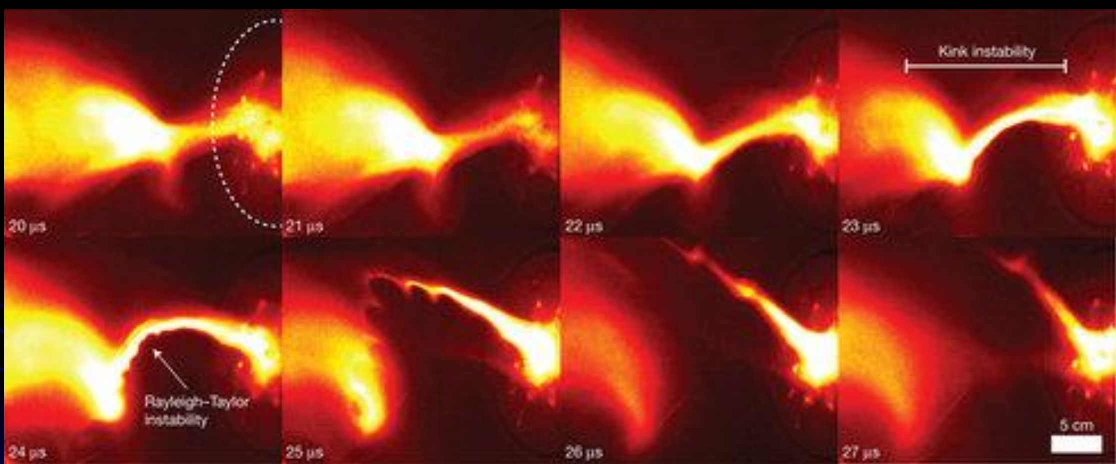

Secondary R-T instability develops due to acceleration in kink unstable flux tube *Moser and Bellan Nature 2012*

Kelvin-Helmholtz instability

- Consider background steady flow $\mathbf{u}_0$
- Flow shear provides free energy for instability

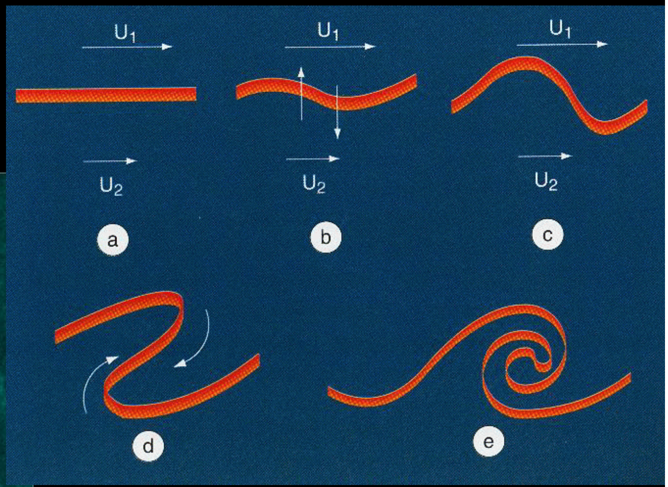

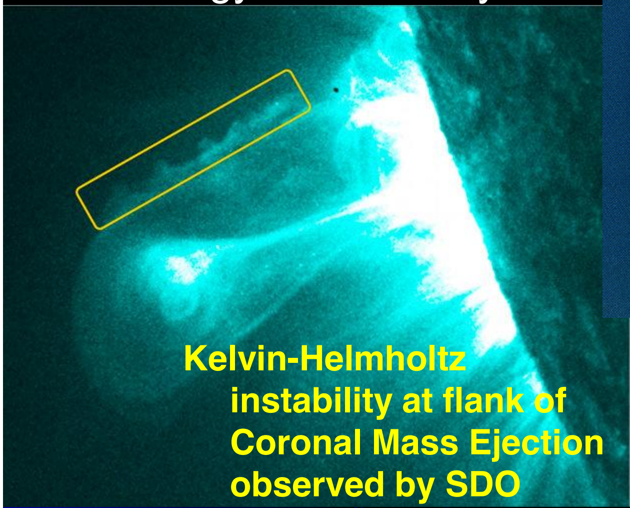

Kelvin-Helmholtz instability at flank of Coronal Mass Ejection observed by SDO

Foullon et al 2011

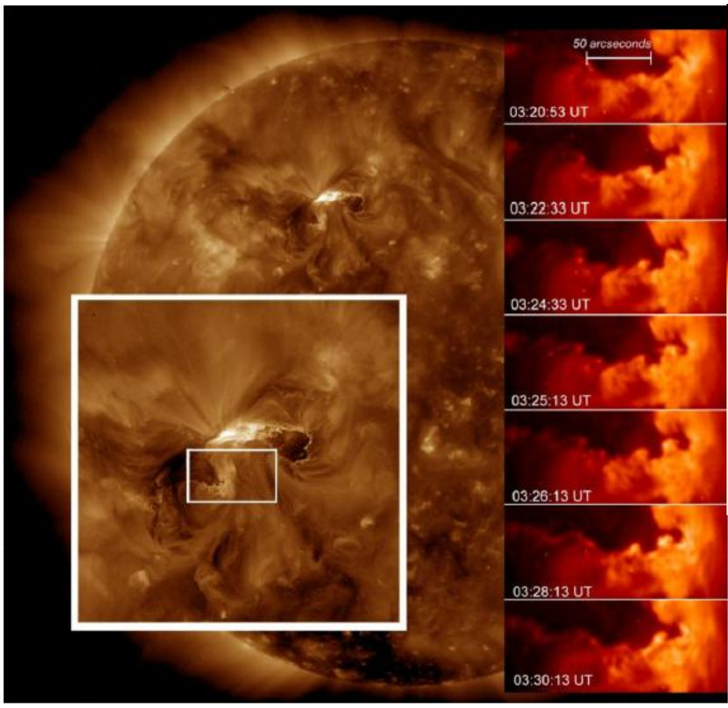

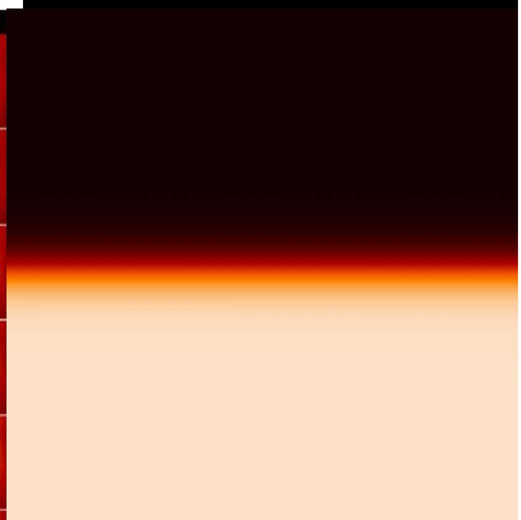

Kelvin Helmholtz instability in CME

Ofman and Thompson 2011

Resistive instabilities and “classical” reconnection models

Magnetic reconnection

- In a **current sheet** there is a strong current **j** in a thin region where the magnetic field **B** changes direction
- Oppositely-directed fields are pushed together by plasma flows – fieldlines “break” and “reconnect” in due to localised dissipative effects
- **Changes magnetic topology** (which is conserved in an ideal – perfectly conducting – plasma)
- **Converts magnetic energy into thermal energy and kinetic energy (bulk flows or non-thermal particles)**

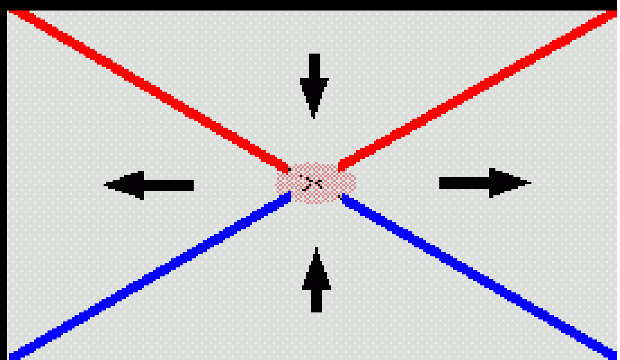

•Outer “ideal” region in which fieldlines are frozen to the plasma

• Localised inner “resistive” or “dissipative” region in which field topology can change

• Much more rapid than Ohmic dissipation

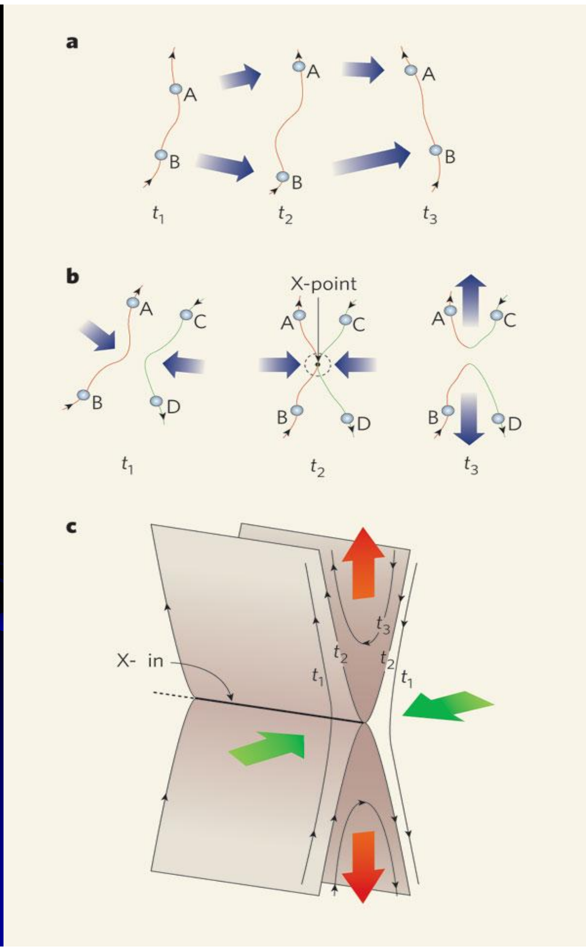

•Flow field interacts with dissipation - non-ideal effects are locally significant even in a highly conducting (large *S*) plasmas

•Associated with reversals in magnetic field (or strong gradients) – occurs at current sheets or null points or other singular layers

"Classical" modes of reconnection

- **Spontaneous reconnection** – linear instabilities of resistive plasma - tearing instability and variants
- **Steady-state reconnection** – continual steady inflow, *Sweet-Parker* and *Petschek* models and variants
- **Forced reconnection** – triggered by external disturbance – *Hahm and Kulsrud*

Tearing instability I

Furth et al, 1963

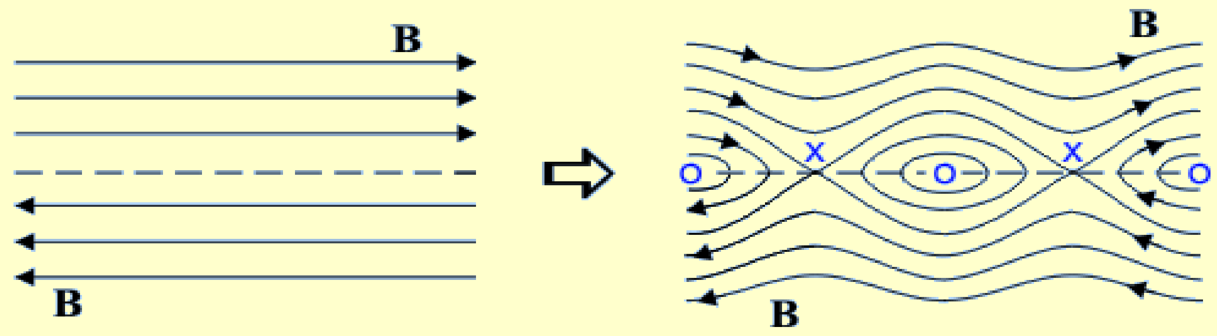

- Tearing mode is a resistive instability – time-dependent reconnection
- Consider an equilibrium current sheet (magnetic field reversal)

e.g. $B_0(x) = B_0 \tanh(x/a)$

or a sheared field $\mathbf{B} = B_{oy}(x)\hat{\mathbf{y}} + B_{0z}(x)\hat{\mathbf{z}}$

- Express B and v in terms of flux function and stream function (incompressiblity assumed)

$$\mathbf{B} = \hat{\mathbf{z}} \times \nabla \psi + B_z \hat{\mathbf{z}}, \quad \mathbf{v} = \hat{\mathbf{z}} \times \nabla \varphi + v_z \hat{\mathbf{z}}$$

Tearing mode II

- Consider small perturbations, assume time dependence $e^{\gamma t}$
- Linearise MHD equations

$$\gamma \psi_1 = \mathbf{B_0}.\nabla \phi_1 + \eta \nabla^2 \psi_1,$$
$$\gamma \nabla^2 \phi_1 = \mathbf{B_0}.\nabla j_1 + \mathbf{B}_1.\nabla j_0.$$

- Inner "resistive" layer – inertia balances resistive diffusion

$$\nabla^2 \phi_1 \approx \phi_1'' \approx \phi_1 / \delta^2 ; \quad \nabla^2 \psi_1 \approx \psi_1'' \approx \Delta' \psi_1 / \delta.$$

where δ is transverse scale of resistive layer

- Match inner solution to outer solution using continuity of Δ' (jump in perturbed flux derivative across resistive layer)

$$\Delta' = \frac{1}{\psi_1(0)} [\psi_1']_{0-}^{0+}$$

Tearing mode III

- Δ' from outer "ideal" region – resistivity neglected, inertia insignificant e.g. for simple field reversal (current sheet)

$$\psi_1 = e^{-k|x|}\left(1+\frac{1}{ka}\tanh\frac{x}{a}\right) \Rightarrow \Delta' = \frac{2}{a}\left(\frac{1}{ka}-ka\right)$$

- Instability if $\Delta' > 0$
- In slab geometry, the most unstable mode has growth rate

$$\gamma \approx 0.6 S^{-1/2} t_a^{-1}$$

occurring at long wavelengths $k \approx 1.4 S^{-1/4}/a$

- Tearing instability growth time is much faster than global resistive diffusion time – intermediate between Alfven and diffusion time-scales - but still slow in the solar corona, where *S* is very large

Steady state reconnection – Sweet-Parker

- Steady inflow driven into current sheet – oppositely-directed fields reconnect in current sheets, reconnected fields emerge in outflow region
- Classic Sweet-Parker reconnection has outflow speed ~ v_A, inflow speed ~ $S^{-1/2} v_A$
- Reconnection timescale $t_{rec} \approx S^{-1/2} t_d \approx S^{1/2} t_a \approx (t_a t_d)^{1/2}$

- Much faster than resistive dissipation – but much slower than Alfven time

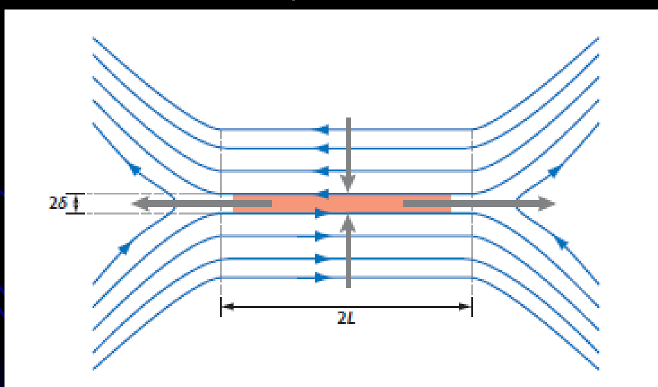

Derivation of Sweet-Parker scalings

Mass continuity: $v_{out} l = v_{in} L$

Ohm's Law (ideal region): $E = v_{in} B$

Ohm's Law +Ampere's Law (inside sheet):

$E = j/\sigma \approx B/\mu_0 \sigma l = \eta B/l$.

$$\Rightarrow v_{in} = \frac{\eta}{l}.$$

Transverse force balance (neglecting velocity since $v_i \ll v_A$):

$$\frac{B^2}{2\mu_0} = p_c - p_e$$

($p_{c,e}$ are pressures at sheet centre/in external region).

Force balance along sheet: $\rho v_y \frac{\partial v_y}{\partial y} = -\frac{\partial p}{\partial y}$

$$\Rightarrow \frac{1}{2}\rho v_{out}^2 = p_c - p_e \Rightarrow v_{out} = \frac{B}{\sqrt{\mu_0 \rho}} = v_A.$$

Combining above equations:

$v_i = v_A S^{-1/2}$

$l = L S^{-1/2}$.

Hence the reconnection timescale $\equiv L/v_i$ is

$$t_r = t_A S^{1/2} = t_d S^{-1/2} = \left(t_d t_A\right)^{1/2}$$

Steady state reconnection: Petschek

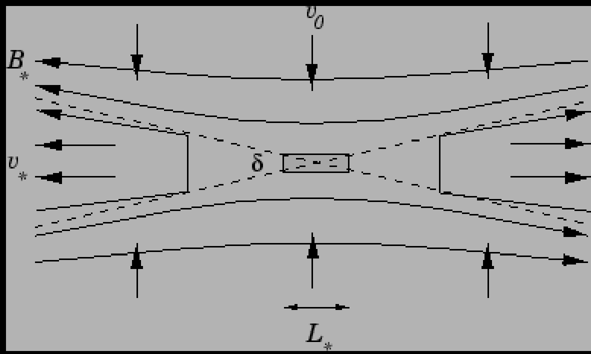

- Even faster steady reconnection is possible e.g. Petschek reconnection which has standing slow mode MHD shock waves in the inflow region
- Shorter current sheet allows for faster reconnection
- Reconnection rate

$$M_e{}^* = \frac{v_i}{v_A} \approx \frac{\pi}{8} \frac{1}{\ln S}$$

Forced reconnection

- A transient external disturbance of the boundary creates a current sheet which subsequently reconnects, dissipating magnetic energy
- Consider a sinusoidal perturbation to the boundary of a 1D slab field with a reversal (*Hahm and Kulsrud, 1985*); or a sheared force-free field (*Vekstein and Jain, 1998*)
- In latter case, a current sheet forms at a resonant surface where $\mathbf{k.B}_0 = 0$
- Energy may be released even if initial field is STABLE to tearing

e.g. Reconnection in a solar coronal loop may be triggered by external disturbance such as displacement of photospheric footpoints

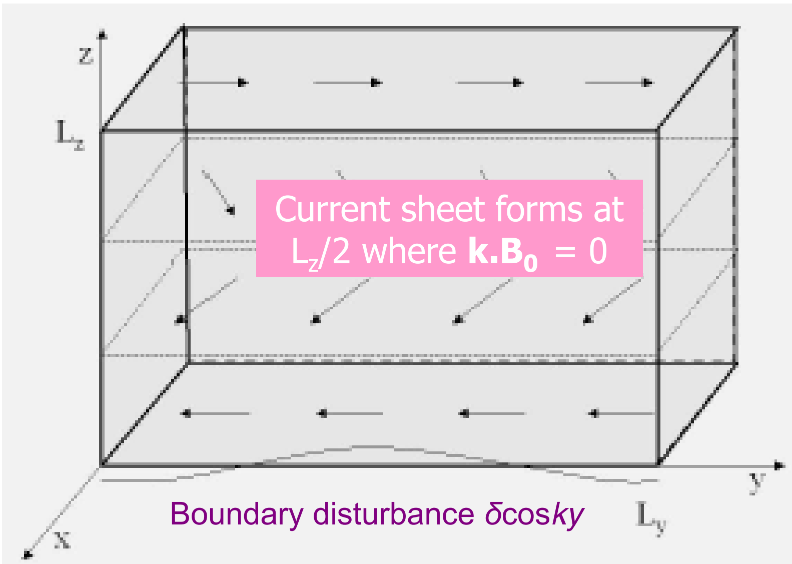

Reconnected and ideal equilibria

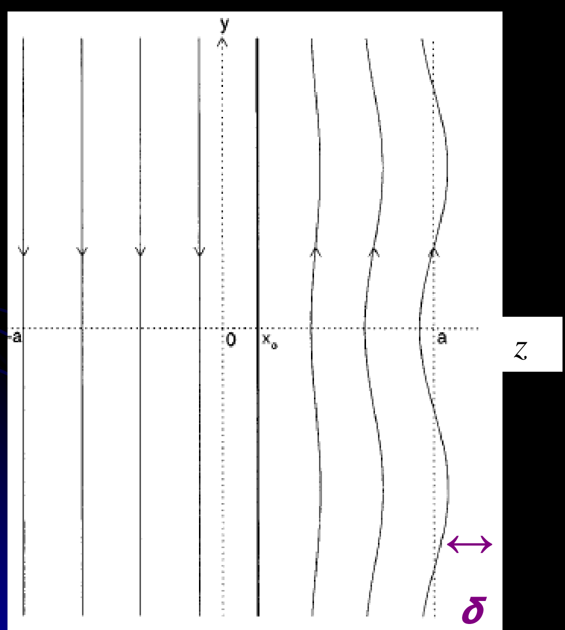

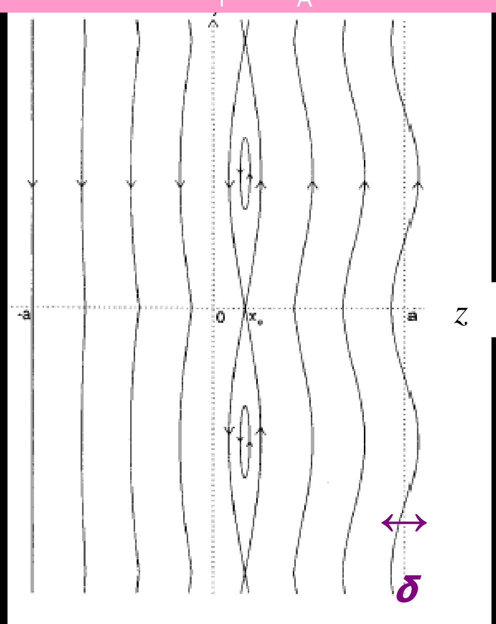

Forced reconnection in reversing field (Harris sheet) *Gordovskyy and Browning, 2010*

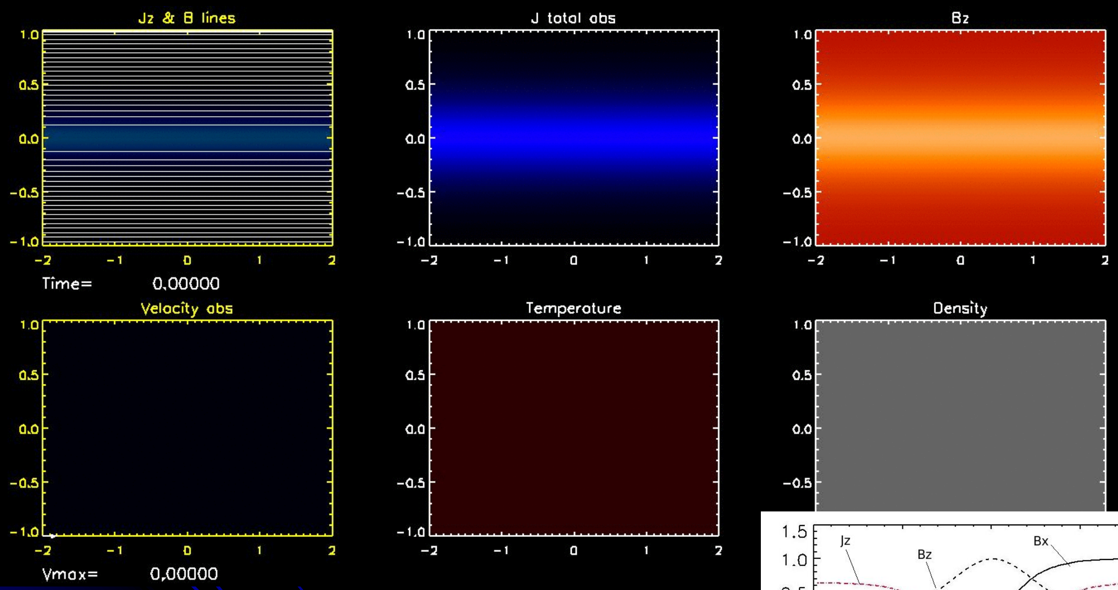

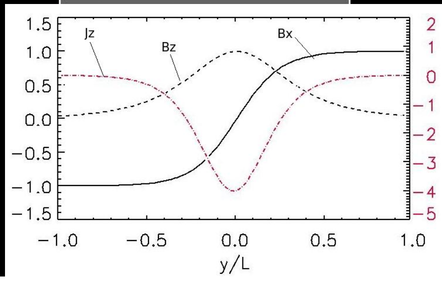

Developments in reconnection modelling

Collisionless reconnection

3D reconnection

Beyond MHD….

- Typical length of coronal loop $10^7 - 10^8$ m (widths of observed loops ≈ 10^6 m) – the global scale length

Take
$$n = 10^{15} m^{-3}, B = 10^{-2} T, T = 10^6 K$$

Lundquist number $S = 10^{14}$

Mean free path
$$\lambda_{coll} \approx 10^4 m$$

Current sheet width in classical MHD tearing theory or Sweet Parker reconnection
$$l \approx S^{-1/2} L \approx 10 - 100m$$

- **MHD valid for global scales but breaks down at local reconnection scales since current sheet smaller than mean free path**
- **MHD reconnection is too slow – look to collisionless models to get faster reconnection**
- **"Dissipation" due to effects other than collisions (Ohmic resistivity)**

Generalised Ohm's Law

- From electron equation of motion, derive generalised Ohm's Law

$$\mathbf{E} + \mathbf{v} \times \mathbf{B} = \frac{1}{ne} \mathbf{j} \times \mathbf{B} - \frac{1}{ne} \nabla . \mathbf{p}_e + \frac{m_e}{ne^2} \left[\frac{\partial \mathbf{j}}{\partial t} + \nabla . (\mathbf{vj} + \mathbf{jv}) \right] + \eta \mathbf{j}$$

- Electron inertia term (*dj/dt*) associated with length-scales of electron skin depth
$$d_e = c / \omega_{pe} = \left(m_e / ne^2 \mu_0 \right)^{1/2}$$
- Hall term (**j** X **B** term) significant on length-scales of order of ion skin depth
$$d_i = c / \omega_{pi} = \left(m_i / ne^2 \mu_0 \right)^{1/2} \qquad \approx 10 \text{ m in corona}$$
- Electron pressure tensor – collisionless dissipation associated with off-diagonal components of electron pressure tensor – non-gyrotropic electrons (Hesse et al, 1999)
- Out of plane field (B_z) – guide field – significantly affects reconnection dynamics

Hall reconnection

- Incorporation of Hall term allows for two-fluid effects – magnetic field frozen to electron fluid
- Hence Hall term is non-dissipative and cannot drive reconnection directly
- Hall term speeds up rate of reconnection – diffusion region develops two-scale structure
- Quadrupolar out-of-plane magnetic fields due to in-plane currents arising from separation of ion and electron flow

From Zweibel and Yamada 2009

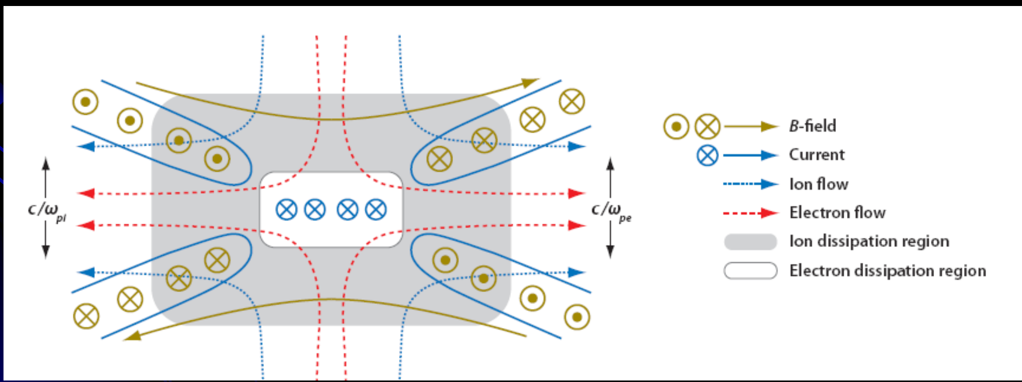

Hall versus MHD

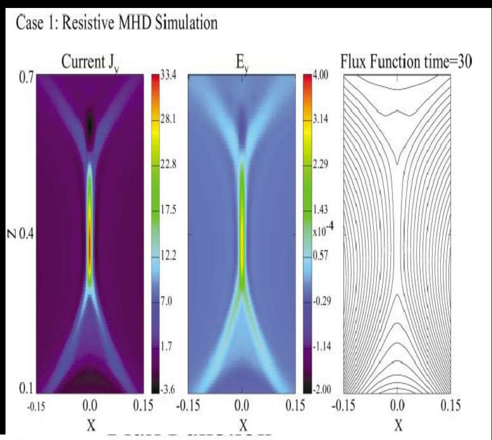

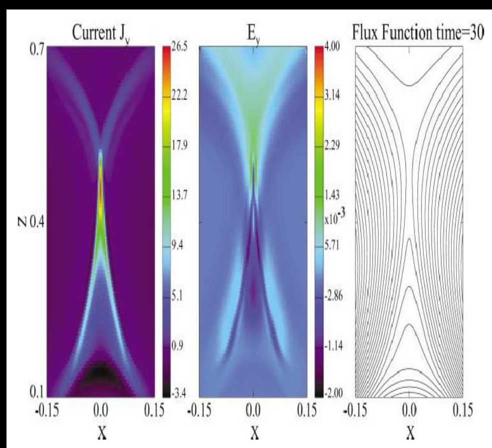

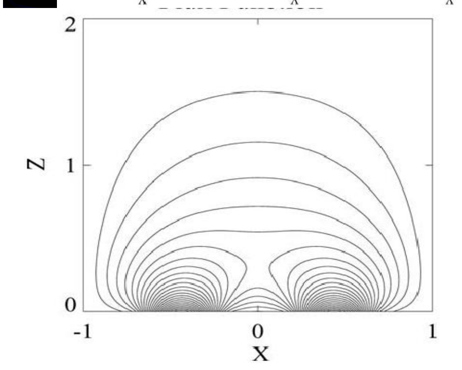

- Simulate reconnection at separatrix with shearing (*Bhattarcharjee, 2004*) for MHD and Hall MHD
- Hall reconnection is more "bursty" – shorter current sheet - scale separation between *j* and *E*

Simulation of collisionless reconnection

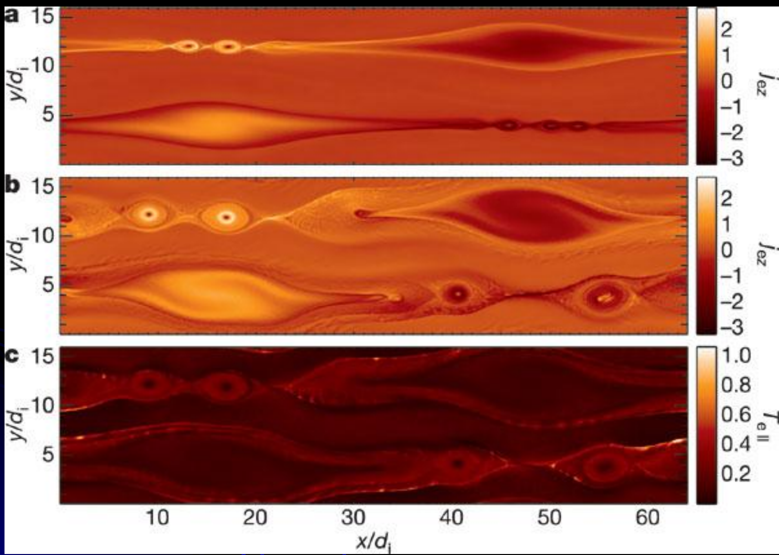

- 3D kinetic Particle in Cell (PIC) simulation of reconnection (from *Drake et al, 2006*)
- Doubly periodic Harris current sheets
- Electron out of plane current at two successive times and temperature

Newton challenge

MHD

Hall

PIC

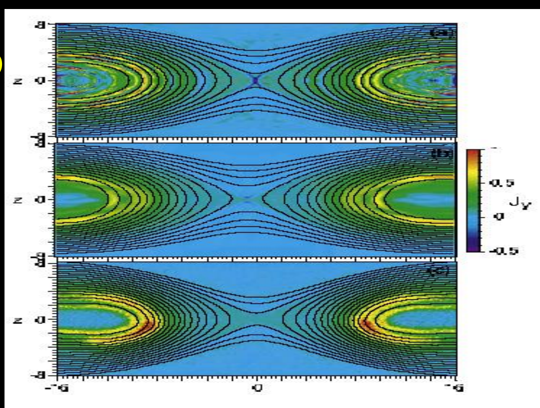

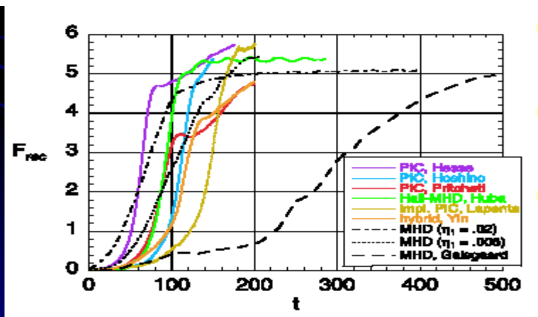

- Typical MHD simulation grid cell ≈ 10^5 - 10^6 m , Typical kinetic simulation box size ≈ 10^3 m
- “Newton challenge” – study forced reconnection in a 1D current sheet (field reversal) using MHD, Hall, PIC codes (*Birn et al, 2005*)
- Localised equilibrium current sheet rather than uniform current
- Final state is close to predicted reconnected equilibrium in all cases
- Reconnection is slower, and resistivity dependent, for pure MHD
- Hall model captures most of dynamics

Reconnection in 3D

2D

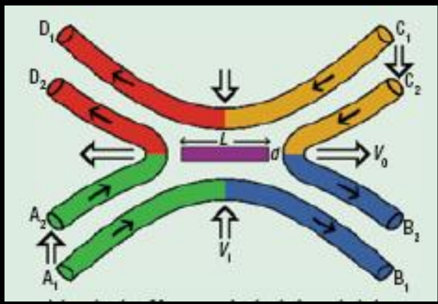

3D

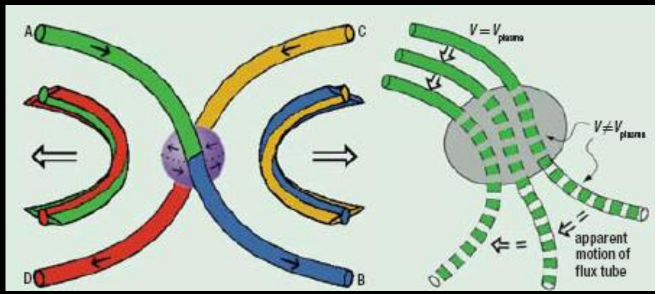

From Cargill et al 2010, Priest et al 2003

- Reconnection in 3D differs in significant respects from 2D (e.g. *Horning and Priest 2003, Priest et al 2003*)
- Reconnection of a pair of flux tubes does not lead to a clearly identified new pair
- Counter-rotating flows in dissipation region
- Apparent flow of fieldlines beyond dissipation region differs from real flow
- Takes place at nulls, separators, quasi-separatrix layers etc

See review *Pontin 2011*

3D reconnection

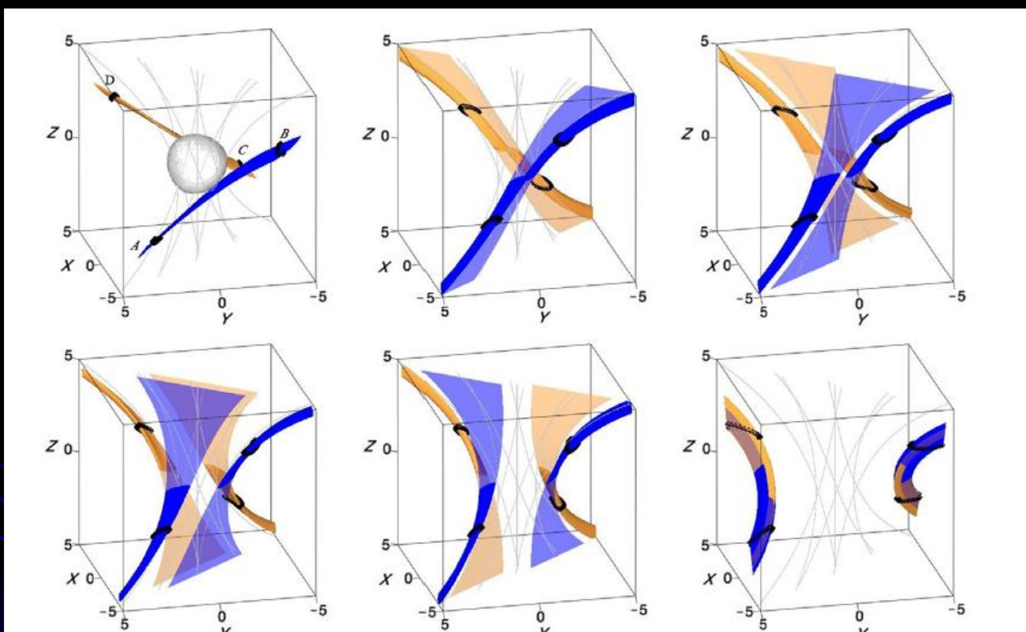

Kinematic model of 3D reconnecting flux tubes with localised resistivity *from Priest et al 2003 and Pontin 2011*

Topology and reconnection sites in 3D

- The "magnetic skeleton" (*Bungey at al, 1996*) comprises:

Field sources, **null points** (B = 0), flux domains (bounded by **separatrix surfaces**) and **separator lines** (intersections of two seperatrices)

- In 3D (or 2D + guide field), reconnection can occur both with and without nulls
- Regions of large gradients in magnetic field line mapping are called Quasi-Separatrix Layers (QSLs; *Titov et al, 2002; DeMoulin 2006*)
  - Squashing factor Q quantifies gradient in field line connectivity
  - A QSL has Q >> 2 (small change in initial field line position leads to very large change in end point location)
  - QSLs are also likely sites for current sheet formation

Reconnection of flux ropes in QSLs in a plasma experiment

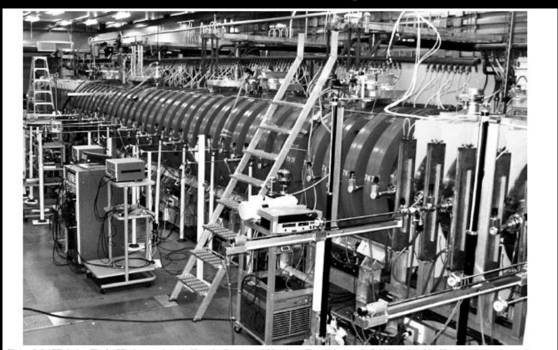

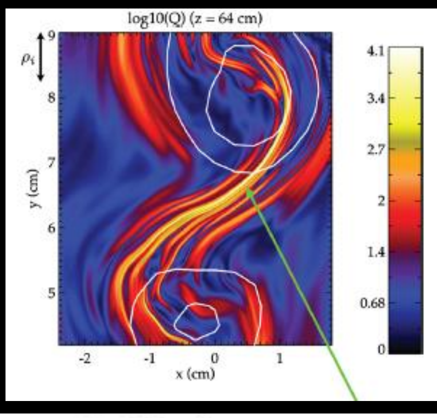

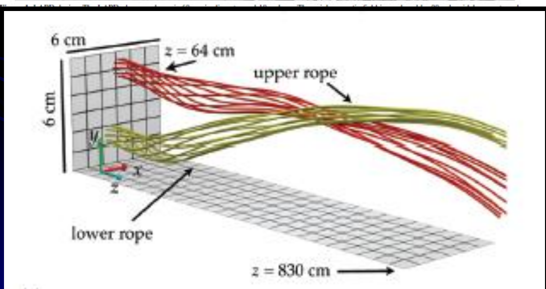

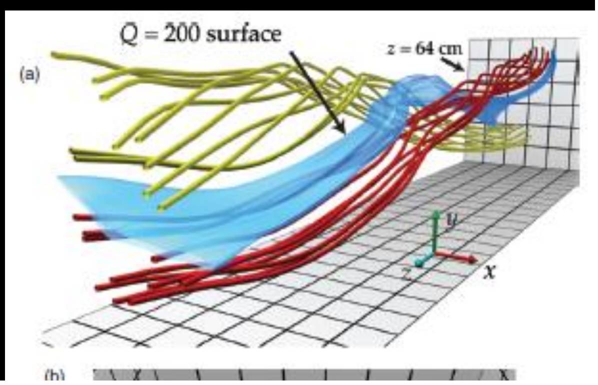

Gekelman et al Ap J 2012

Reconnection at 3D null points

- Field near a 3D null ($B = 0$) has a spine line and a fan surface (Lau and Finn, 1990; Priest and Titov, 1996) – analogue of separatrix lines in 2D
- Priest and Titov (1996) present a "kinematic" model which represents outer ideal inflow/outflow regions
- For self-consistent models incorporating inner resistive region see e.g. Craig et al (1997)

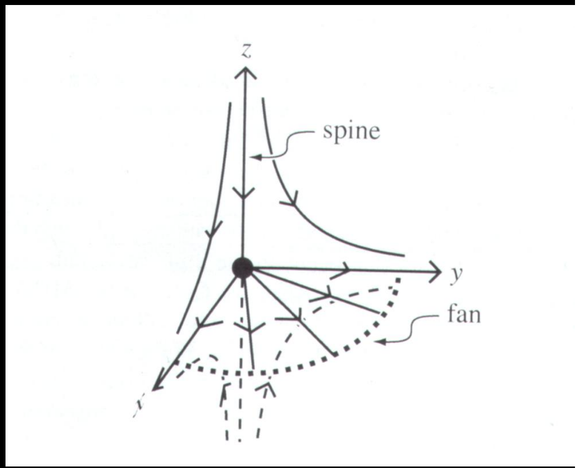

$$\mathbf{B} = B_0 \frac{R}{L} \mathbf{e}_R - 2 B_0 \frac{z}{L} \mathbf{e}_z$$

Spine and fan reconnection

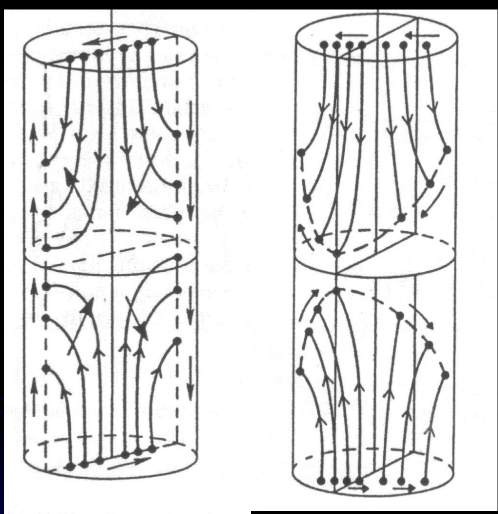

from Priest and Titov, 1996

Spine – singular current at spine line

Fan – singular current at fan plane

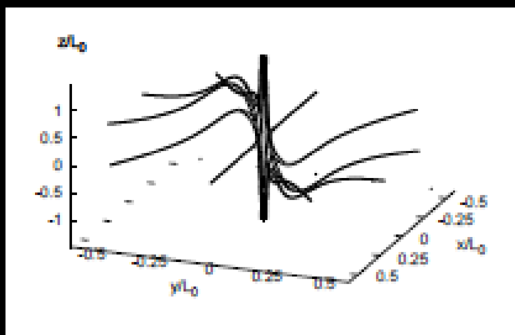

- Spine reconnection fieldlines based on Craig et al 1997
- Solution of steady 3D MHD equations
- Compression of spine field lines, bending of fan plane – current sheets of finite length along spine

3D reconnection in pair of twisted flux tubes,

De Moortel and Galsgaard, 2006

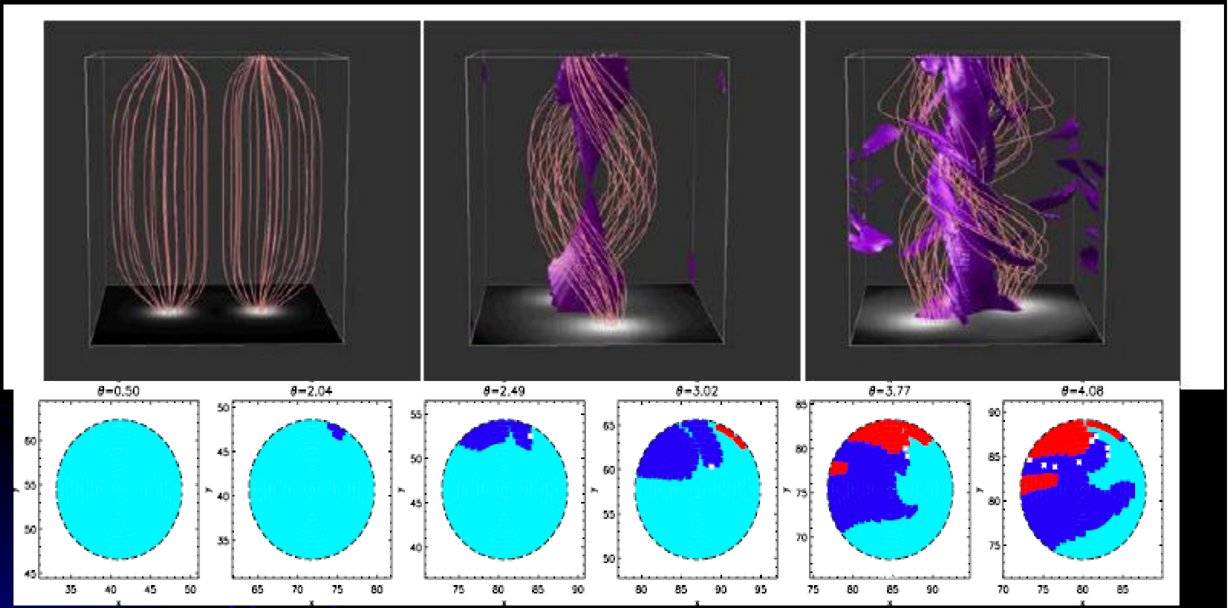

Field with original connectivity

Field reconnected to other source

Field leaving box

Reconnection in the corona and coronal heating

Solar coronal heating

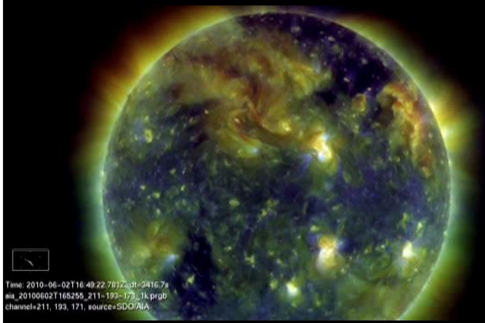

SDO

TRACE

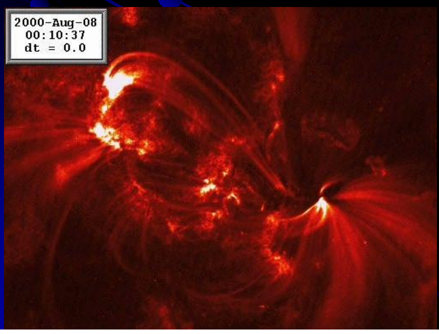

- To maintain the coronal plasma at millions of degrees, need heat source to balance conductive and radiative energy losses (up to 10^4 Wm $^{-2}$ in Active Regions)
- Heating is associated with magnetic field – energy input from photospheric motions
- Depending on timescale of driving motions, heating may be associated with damping of waves (“fast”) or quasi-steady currents (“slow”)
- Slowly twisting or shearing the footpoints of the coronal field stores free magnetic energy (currents) in force-free equilibrium j **XB = 0**

Coronal energy storage and dissipation

Energy input from photosphere is sufficient

$$F = |\mathbf{E}\times\mathbf{B}/\mu_0| = B_v B_h v_{phot} / \mu_0 \approx 10^4\, Wm^{-2}$$
$$(B \approx 0.01T, B_h \approx 0.1B, v_{phot} \approx 1kms^{-1})$$

•Magnetic reconnection is a strong candidate for efficient dissipation of the stored energy
→ coronal heating may be due to combined effect of many small flare-like events “nanoflares”
•Reconnection sites (current sheets) should be common in complex coronal field

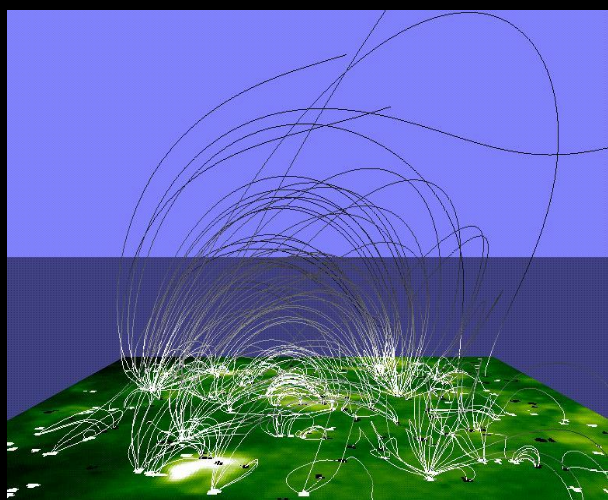

Origin of current sheets in the corona I

- **Simple field, complex footpoint motions**
- Parker (1972, 1983) proposed asymmetric braiding motions of the photospheric footpoints of straight uniform coronal loop leads to lack of equilibrium

→ Singularities (current sheets) must form

- Still controversial – seems more likely that 3D equilibria can exist but finite strong currents develop

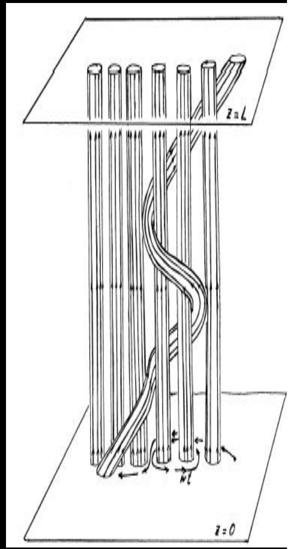

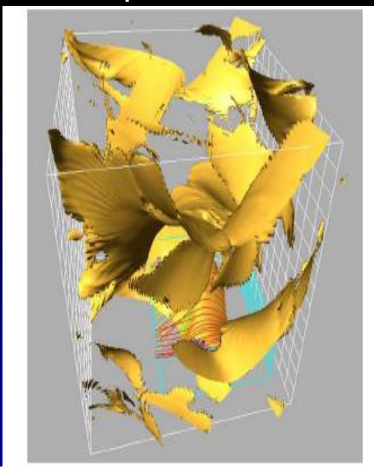

Current isosurface from numerical simulation of flux tube braiding (*Galsgard and Nordlund, 1996*)

Origin of current sheets in the corona II

- **Complex field topology, simple motions**
  - Footpoint displacements in fields with nulls, separatrices, separators, QuasiSeparatrix Layers
  - Coronal field with discrete photospheric flux sources
  - Emerging flux
- **Simple fields, simple motions**
  - Disturbance of resonant surface (forced reconnection)
  - Nonlinear kink instability

From Longcope, 2001

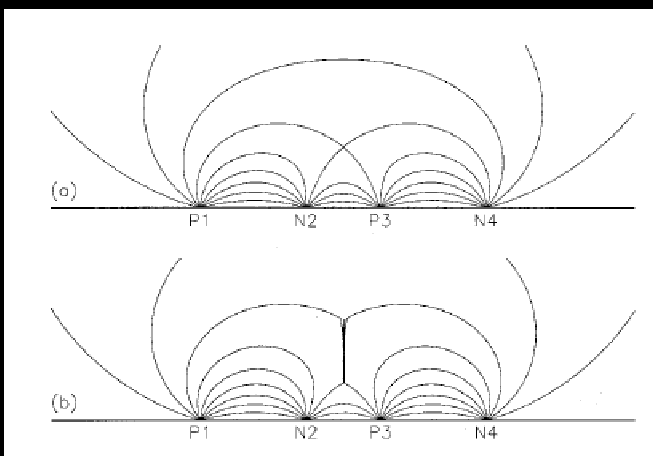

Magnetic helicity

- Magnetic helicity

$$K = \int_V \mathbf{A}.\mathbf{B}dV \qquad (\nabla \times \mathbf{A} = \mathbf{B})$$

Measures degree of self-linkage or twistedness of the magnetic field

- For two flux tubes K =2$\varphi_1\varphi_2$ if tubes interlink, K = 0 if no interlinkage
- For twisted flux tube K = Tφ^2 where T is the twist (=1/q = number ot timed field line turns in one toroidal circuit)
- Modify in region with flux crossing boundary to ensure gauge-invariance (*Finn and Antonsen, 1985)*

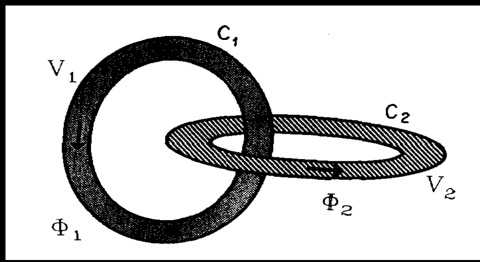

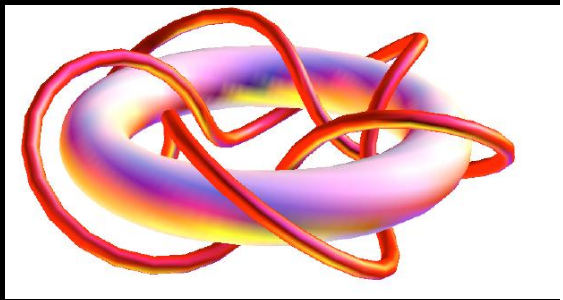

Fieldline links toroidal flux 5 times

From *Berger (2000)*

Helicity and reconnection

•Global magnetic helicity conserved during magnetic reconnection

•Helicity may be converted between linkage and twist but created/destroyed (in closed region)

•Dissipated only on long Ohmic time-scales (t_d) -much more slowly than magnetic energy - helicity dissipation is very slow in the solar corona (*Berger, 1984)*

$$\frac{dW}{dt} = -\int_{vol} \eta \mathbf{j}.\mathbf{j}dV \approx -\eta B^2 L^3 / \mu_0^2 l^2 , \frac{dK}{dt} = -2\int_{vol} \eta \mathbf{j}.\mathbf{B}dV \approx -2\eta B^2 L^3 / \mu_0 l$$

$$\Rightarrow \frac{(\Delta K / K)}{(\Delta W / W)} \approx \frac{l}{L} << 1$$

assuming dissipation occurs in thin current sheets of width l << L (global length scale)

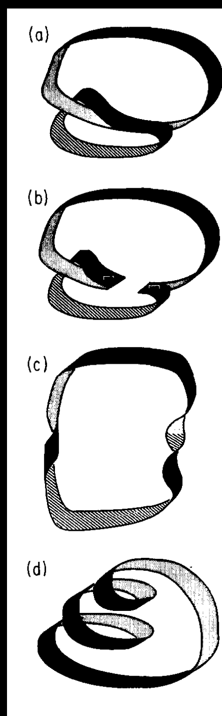

From Pfister and Gekelman, 1991)

Relaxation and minimum energy states

- How can we calculate the energy release due to multiple reconnection events in a complex field?
- The field relaxes to a state with minimum magnetic energy - subject to the appropriate constraint for a highly conducting plasma: total magnetic helicity is conserved *(Taylor, 1974)*
- The minimum energy state is a constant-*α* (linear) force-free field

$$\nabla \times \mathbf{B} = \alpha \mathbf{B}$$
$$\alpha = \mu_0 \mathbf{j}.\mathbf{B} / B^2 = \text{constant}$$

- This is a special case of a force-free field **j** X**B** = **0** which can be expressed

$$\nabla \times \mathbf{B} = \alpha(\mathbf{r})\mathbf{B}$$

Relaxation and solar coronal heating

- Helicity is injected by twisting and shearing of photospheric footpoints

$$\frac{dK_{rel}}{dt} = -2 \int_{photosphere} \mathbf{A}_0 . \mathbf{v}\, \mathbf{B}.d\mathbf{S}$$

- Stressed field relaxes to a constant-α state – energy released, helicity conserved

(*Heyvaerts and Priest, 1984; Browning, 1988*)

- Excess energy over minimum energy state dissipated as heat → coronal heating
- Process repeats: stress-relax, stress-relax,….- gives distribution of heating events (*Bareford et al 2010, 2012*)

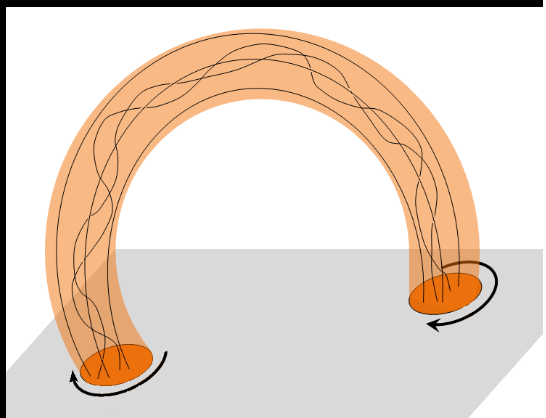

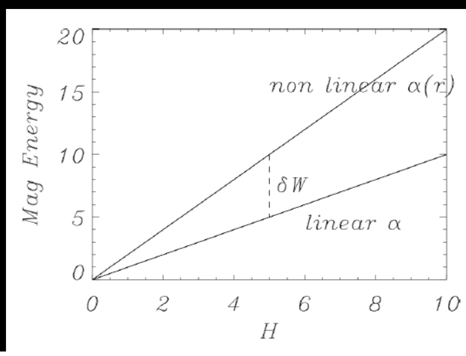

How does relaxation work in the corona?

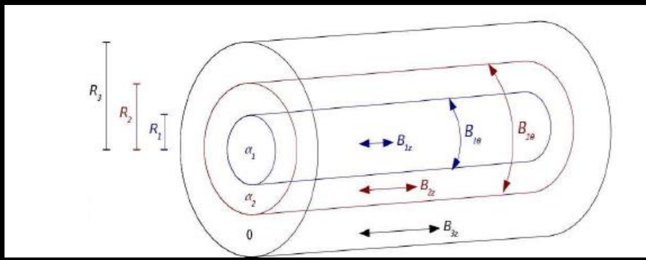

Numerical simulations of non-linear kink instability in cylindrical loop using LARE3D code (*Arber et al 2001)*

– initially in kink linearly-unstable equilibrium with α(r) profile

$$\alpha = \alpha_1\,,\quad r < R_{c;}$$
$$\alpha = \alpha_2\,,\quad r > R_c$$

Browning and Van der Linden, 2003; Browning et al, 2008; Hood et al 2009

Current sheets develop in nonlinear phase of ideal kink instability
→fast reconnection

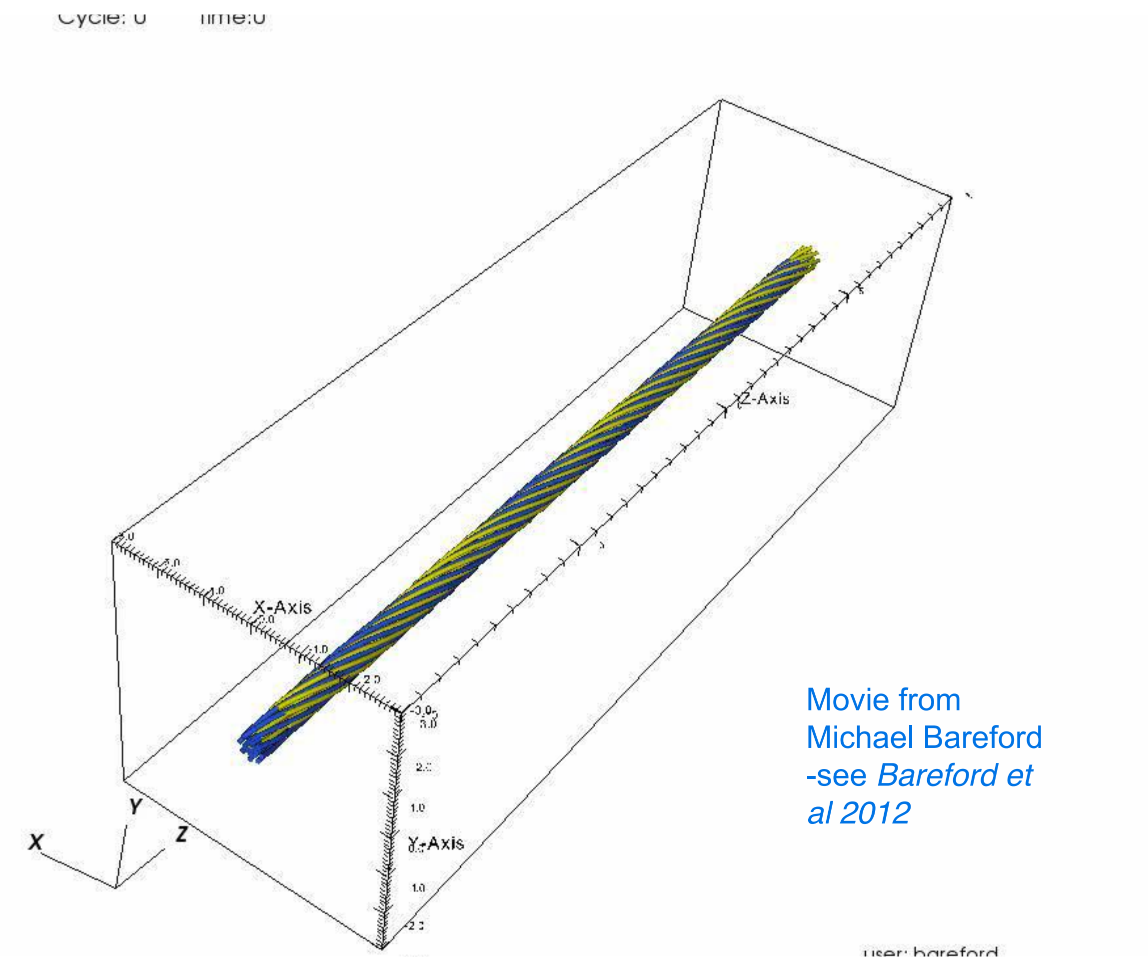

Movie from Michael Bareford -see *Bareford et al 2012*

Reconnection in kink unstable loop

- midplane at successive times Hood et al, 2009

Current |j| and velocity vectors

Temperature

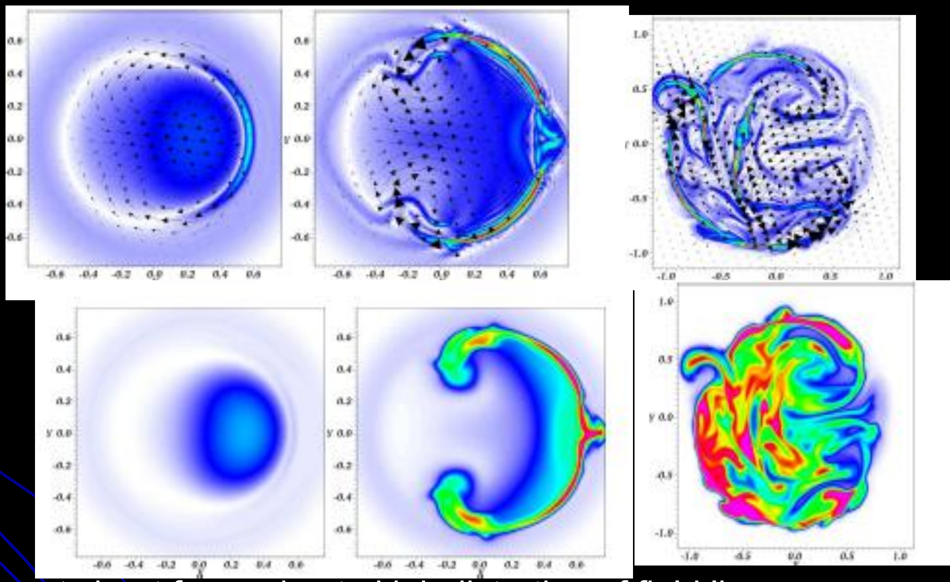

- Helical current sheet forms due to kink distortion of field lines
- Stretched and fragments leading to multiple reconnection and distributed heating
- Relaxes to near-equilibrium with reduced energy – close to constant-α

Reconnection in action: jets in solar atmosphere

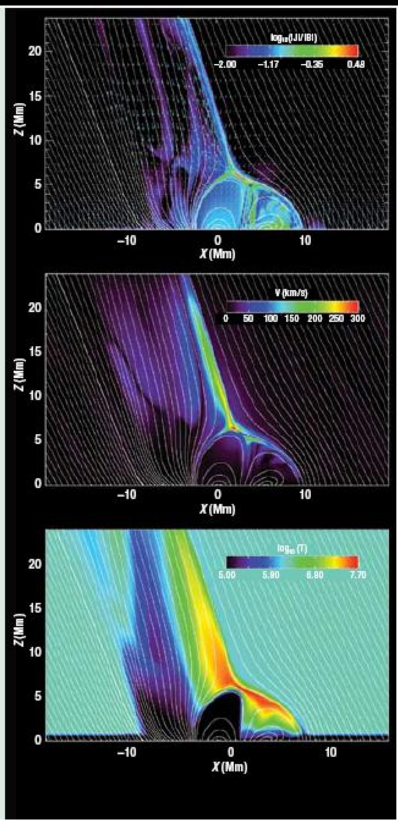

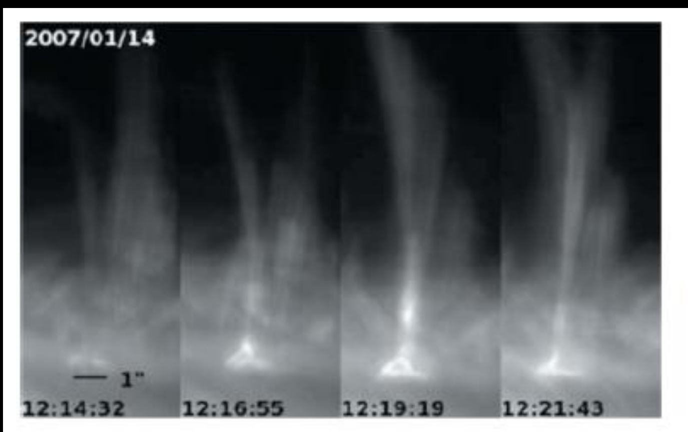

- 3D MHD simulations of new flux emerging into solar corona – with jet (*Moreno-Insertis et al 2008*)
- Anemone jets in chromosphere from Hinode (*Shibata et al 2007*)

Emerging flux simulation

Archontis et al, 2005

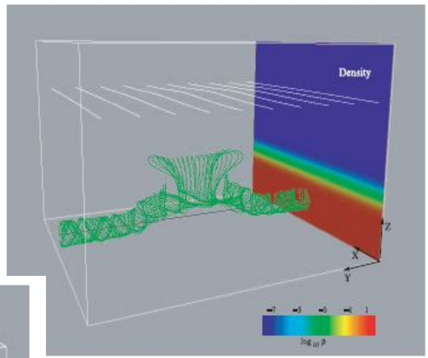

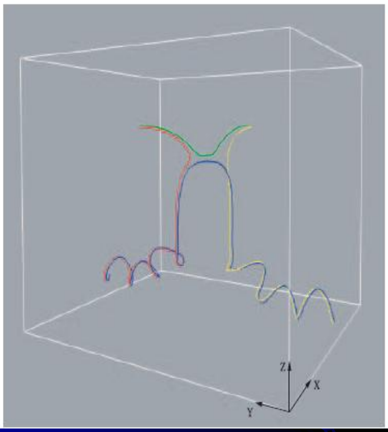

Twisted flux tube emerges from below surface into pre-existing coronal field –

Reconnects with overlying field

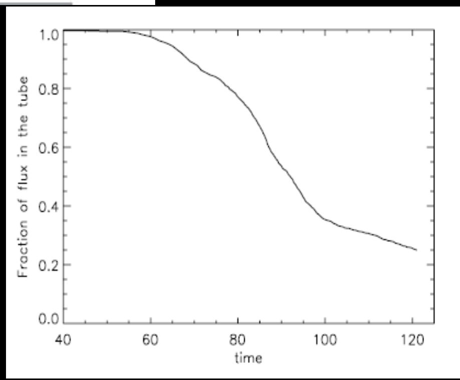

Emerging flux: 3D reconnection and null points

- 3D MHD simulation of emerging flux (*Archontis et al 2004*)
- Leads to compex topology
- Magnetic separators (black line) + regions of strong electric field (green) + magnetic null points (red and blue) - from *Maclean et al 2009*

Reconnection and particle acceleration in solar flares

Examples of reconnection: flares

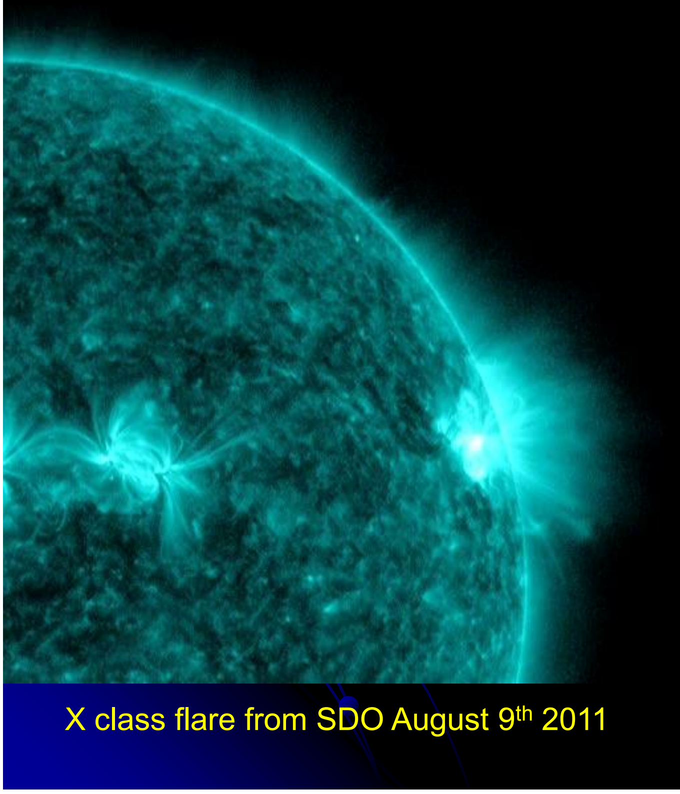
X class flare from SDO August 9th 2011

- Solar flares are dramatic events releasing up to 10^{25} J of stored magnetic energy over a period of hours – strong brightening in soft x-rays
- Flares generate plasma heating and fast particle beams - signatures across the em spectrum from gamma rays to radio
- Primary energy release process believe to be magnetic reconnection

Canonical flare model

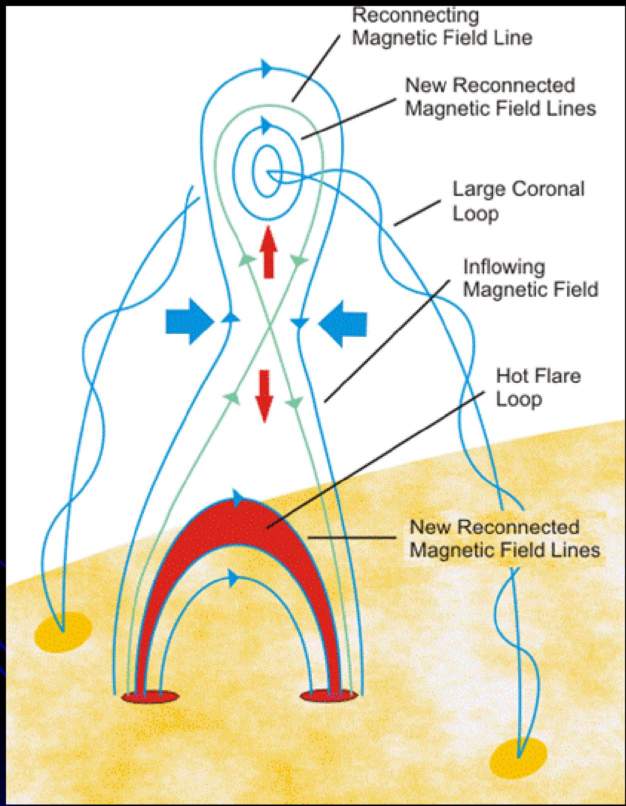

Release of stored magnetic energy by magnetic reconnection

from Tsuneta 1996 and much previous work

High energy particles in flares

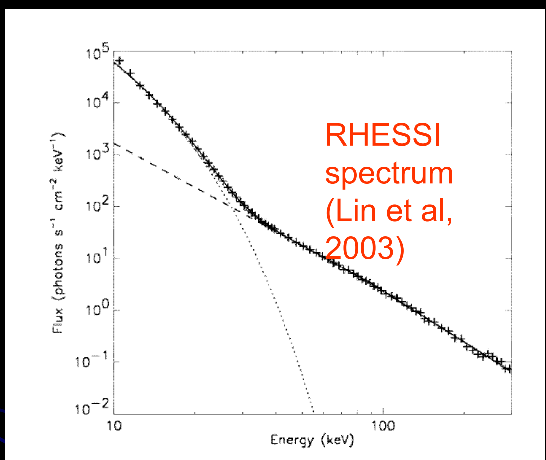

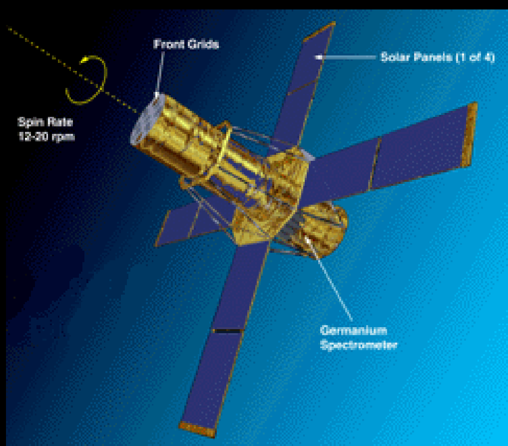

- High energy particles detected *in situ* by particle detectors in space and indirectly near Sun through radiation
- Emission from flares shows both thermal and non-thermal components (hard x-rays, gamma rays) due to Bremstrahlung of electrons and nuclear reactions/excitations of ions

Particle acceleration mechanisms

- Since reconnection is primary energy release mechanism, it is plausible that electric fields associated with reconnection may accelerate charged particles
- Other acceleration mechanisms are proposed – turbulence, plasma waves, shocks, collapsing magnetic traps – also variants of reconnection acceleration (e.g. multiple reconnection sites) and hybrid mechanisms
- Require to explain electron energies of up to ≈ 1 MeV, proton energies of up to ≈ 1 GeV – or higher in gamma ray flares; acceleration times of ≈ 1s or less
- Studying charged particle energy spectra, spatial distribution etc may provide information about reconnection site geometry and parameters

Electric fields in flares

- Flare electric fields can be estimated from flux conservation arguments (**E** = -**v** X **B**), from observed motion of "ribbons" (footpoints of flare loop) - estimate electric fields of around 1000 Vm^{-1}
- The Dreicer electric field is the critical value of E above which electrons are freely accelerated as in a vacuum (Coulomb collisions are insignificant)
  - Coulomb collision rate is a decreasing function of velocity (temperature) – fast electrons have few collisions

$$E_d = \frac{e \ln \Lambda}{4\pi\varepsilon_0 \lambda_D^2} \propto \frac{n}{T} \quad \left(\lambda_D = \sqrt{\frac{\varepsilon_0 kT}{ne^2}}, \text{ the Debye length; } \ln\Lambda \approx 20 \right)$$

- Typical flare electric fields are super-Dreicer ($E_d \approx 0.01 Vm^{-1}$)
- Particles may thus gain significant energies if directly accelerated along the electric field for long enough

  e.g. acceleration by E = 1000 Vm^{-1} over 10,000 km gives energy 10 GeV

Particle trajectories in reconnecting fields

- Magnetic field inhibits acceleration – particles drift if **E** perpendicular to **B**
- Reconnection electric field transverse to current sheet – may also be magnetic field components perpendicular to sheet ($B_\perp$), small, and parallel to electric field ($B_{//}$)
- Particles are brought into current sheet by **E** X **B** drift
- Within sheet they gyrate around $B_{//}$ and are accelerated along electric field – until ejected from sheet gyromotion associated with $B_\perp$
- Energy gain depends on time spent in sheet (distance travelled along sheet)

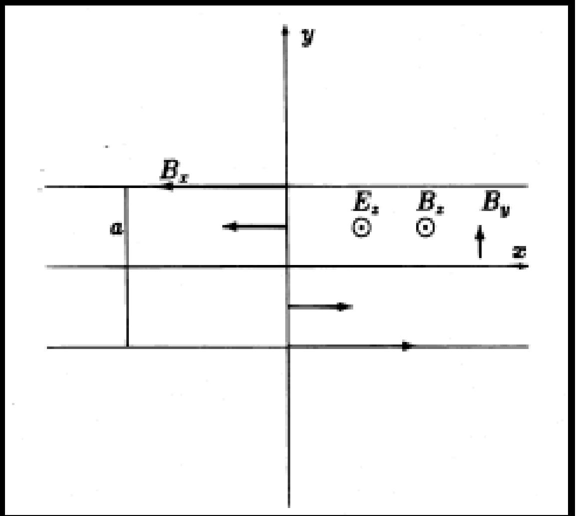

Consider X-point (neutral point) or current sheet geometry

Test particle approach

- Charged particle behaviour in non-uniform electromagnetic fields – especially in reconnecting fields with magnetic null points or reversals – is far from fully understood!
- Take magnetic and electric field configuration representative of reconnection e.g. from analytical model
- Neglect the fields generated by the test particles (ok if number of high energy particles is few compared with “background” plasma which generates electromagnetic fields)
- Usually neglect collisions of test particles with the background plasma
- Integrate equations of motion numerically – Lorentz equations or guiding-centre

$$\frac{d\mathbf{x}}{dt} = \frac{\mathbf{p}}{m\gamma}$$
$$\frac{d\mathbf{p}}{dt} = q\left(\mathbf{E} + \frac{1}{c}\frac{\mathbf{p}}{m\gamma} \times \mathbf{B}\right)$$

2D test particle models

- X-point or current sheet configuration
- Invariance of all quantities in the 'z' direction
- May include a "guide field" B_z
- A large number of studies published....

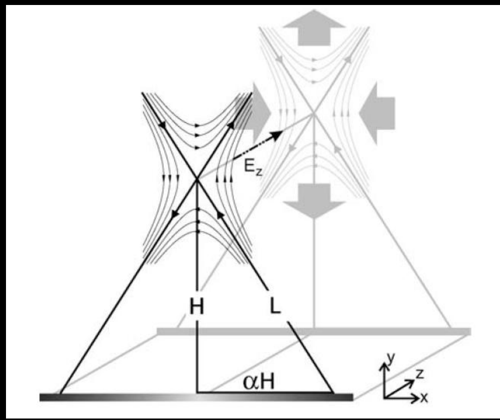

Hannah & Fletcher, 2006

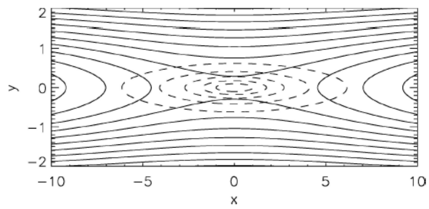

Wood & Neukirch, 2005

Figure 1. An example of the field configuration used in this paper (using $L = 10$). Note that for graphical reasons the configuration is not shown with the correct aspect ratio, so that it is actually a lot more elongated in the x-direction than shown here. The *solid lines* are projections of magnetic field lines onto the x–y plane (contours of the flux function A). The non-ideal region in which a field-aligned component of the electric field exists is outlined by the *dashed contours*.

Results of 2D test particle models

- Efficient acceleration is possible, provided the electric field is strong enough to allow efficient drift towards the null point / current sheet.
- Energy gain strongly dependent on a particle's initial position
- Presence of a guide field results in more efficient acceleration, also separates species

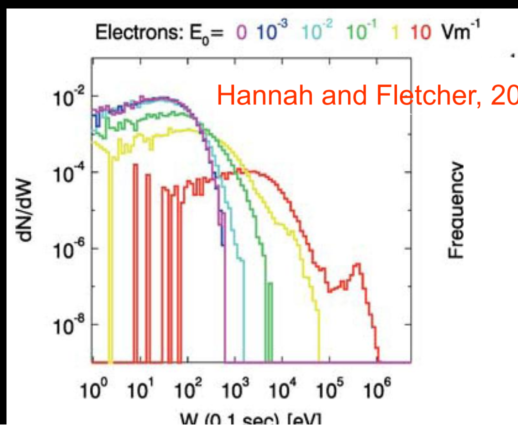

Hannah and Fletcher, 2006

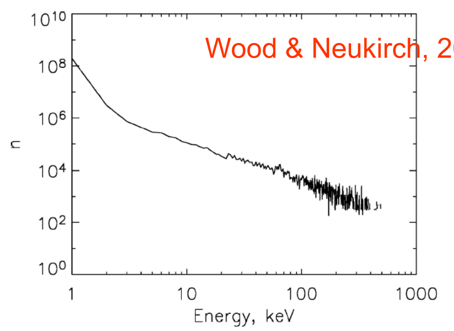

Wood & Neukirch, 2005

3D null points in flares

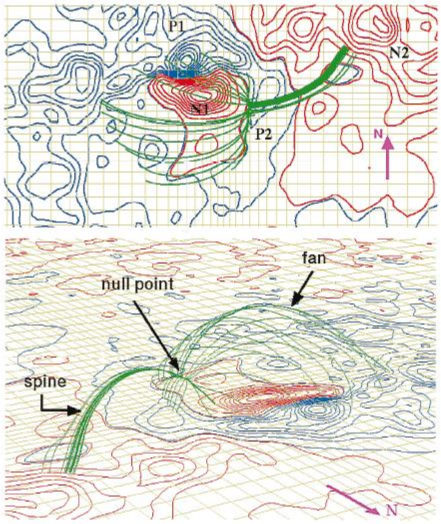

Aulanier et al (2000)

3D null points

(B = 0)

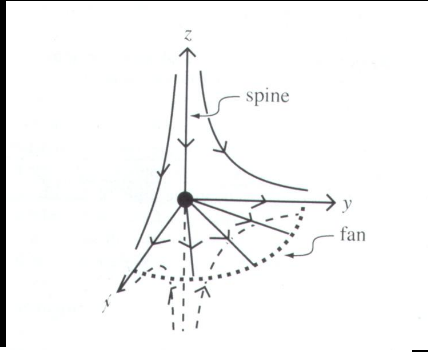

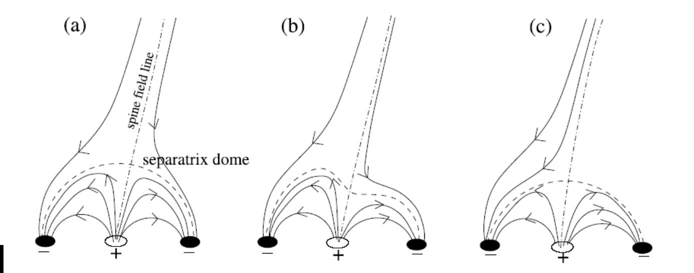

Fletcher et al (2001)

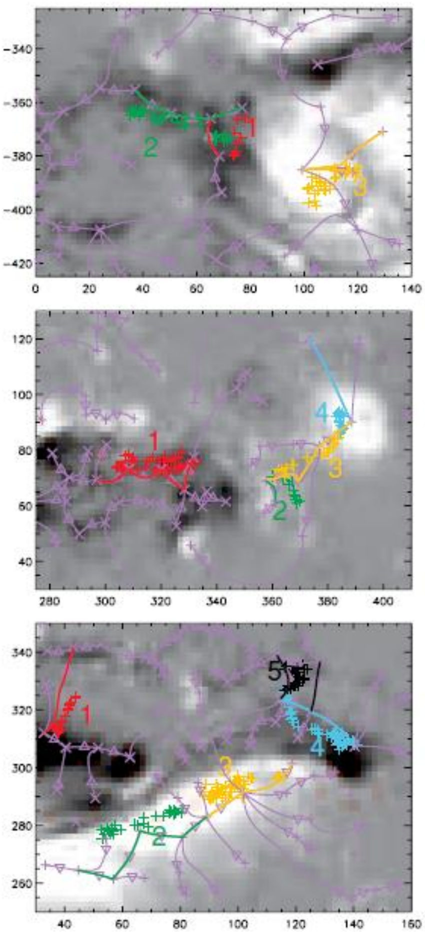

Reconnection in action – 3D nulls in the corona

Spine lines and Hard X-ray footpoint sources from 3 flares

Desjardins et al 2009

Particle acceleration at 3D null points

- Inject test particles into electromagnetic fields representing analytical solutions of MHD equations at 3D reconnecting nulls *(e.g. Priest and Titov 1996, Craig et al 1997)*
- Current sheets may develop at spine line or fan plane – also electric fields associated with inflow – can acccelearte particles to high energy

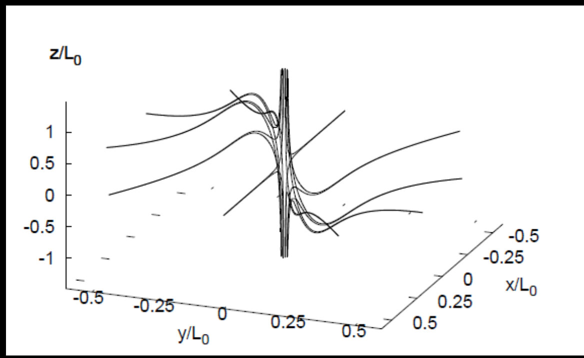

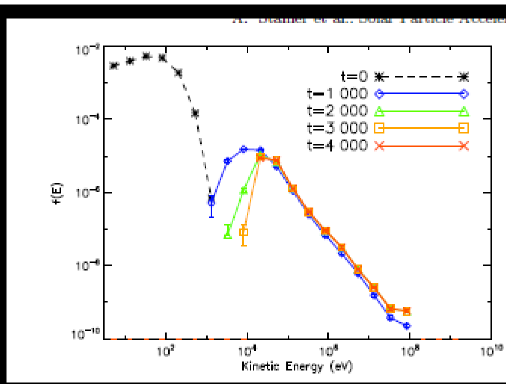

Stanier et al A & A 2012

See also Dalla and Browning 2005, 2006; Browning et al 2010

Test particles in kink-unstable twisted loop

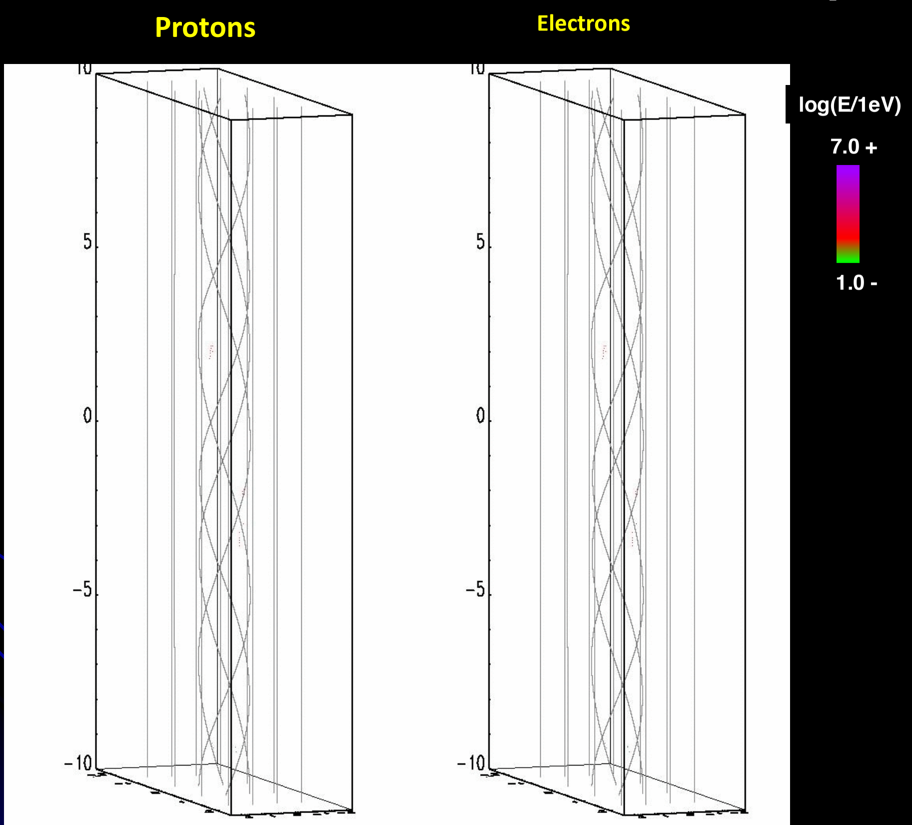

Particles accelerated by electric fields in fragmented current sheet

Gordovskyy and Browning ApJ 2011, Sol Phys 2012

Test particles in kink-unstable twisted loop

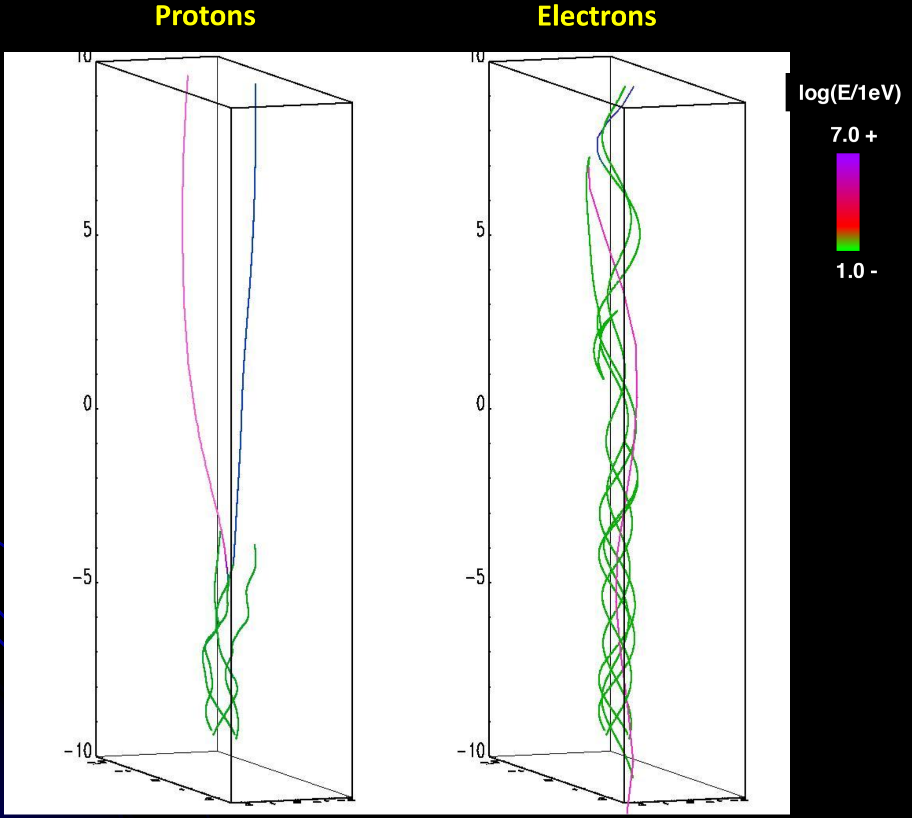

Particles accelerated by electric fields in fragmented current sheet

Gordovskyy and Browning ApJ 2011, Sol Phys 2012

Particle distribution in space

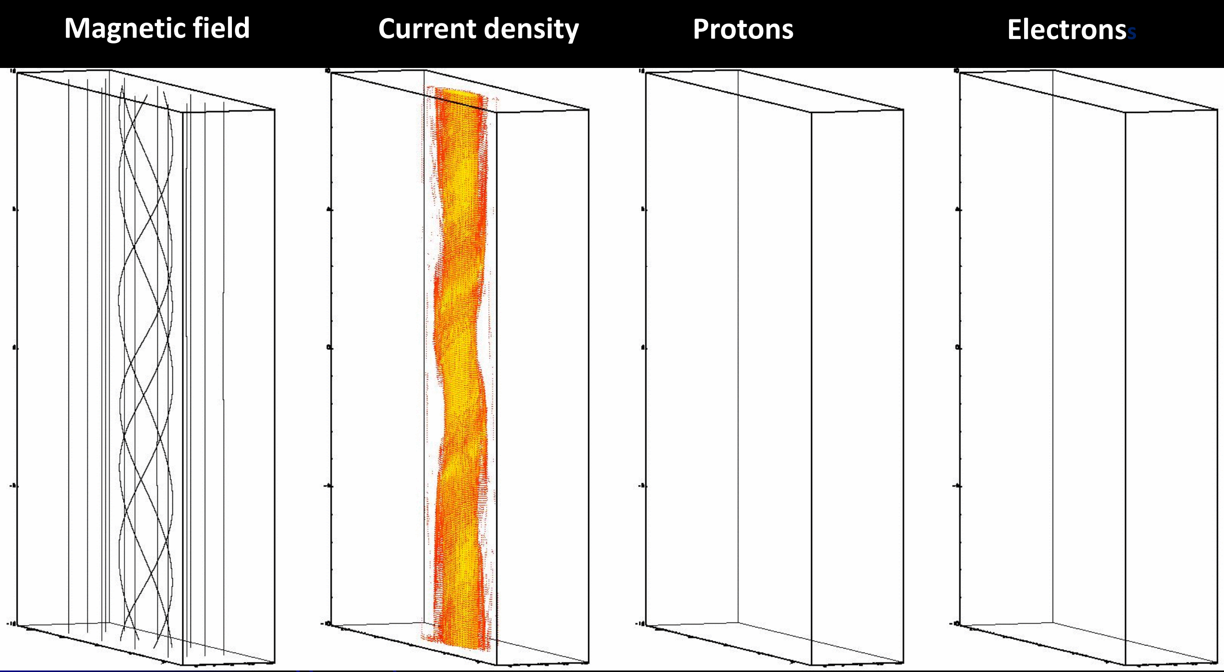

E = 100keV...1MeV
E > 1MeV

Particle distribution in space

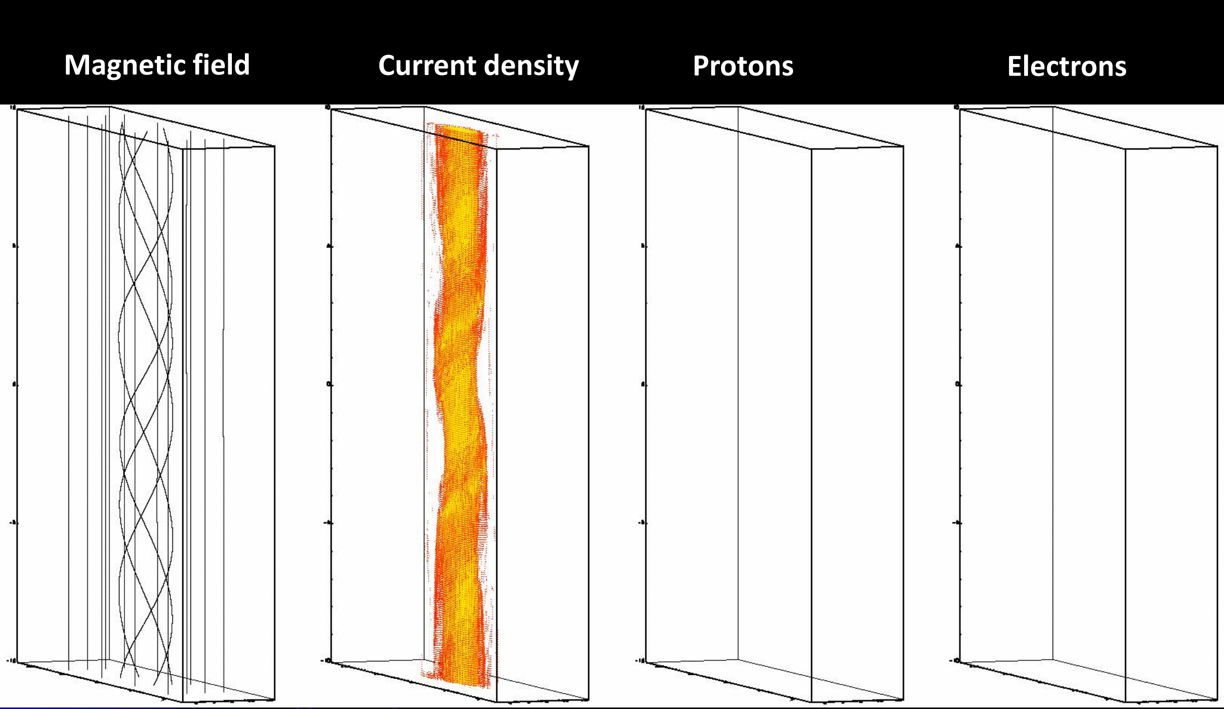

E = 100keV...1MeV
E > 1MeV

Reading list

- “Magnetic reconnection” Priest and Forbes (Cambridge University Press, 2000)
- “Magnetic reconnection in plasmas” Biskamp (CUP,2000)
- “Reconnection of magnetic fields” eds. Birn and Priest (CUP 2007)
- “An introduction to plasma astrophysics and MHD” Goossens (Kluwer, 2003)
- “Principles of MHD: with applications to laboratory and astrophysical plasmas” + “Advanced MHD” Goedbloed and Poedts (CUP, 2004, 2010)
- “Physics of space plasma activity” Schindler (CUP 2007)
- “Heliophysics” Vols 1-3 Shrijver and Siscoe (CUP 2010)

Selected references

Apologies for any omissions – for more complete reference list, see recommended books

- Archontis,V. et al (2004)
- Bareford,M. et al *Astron. Astrophys.* 521, A70 (2010)
- Berger,M.A. *Geophys. Astr. Fluid Dyn.* 30, 79 (1984)
- Birn,J. et al, *Geophys Res Lett* 32, L016105 (2005)
- Bhattarcharjee,A. *Ann Rev Astron Astrophys* 42, 365 (2004)
- Browning,P.K. et al, *Astron. Astrophys.* 485, 837 (2008)
- Browning,P.K. et al *Astron. Astrophys* 520, A105 (2010)
- Craig,I.J.D. et al, *Ap. J,* 485, 383 (1997)
- Dalla,S. and Browning,P.K. *Ap. J.Lett*, 640, L99 (2006)
- Desjardins,A. et al. *Ap.J.* 693, 1628 (2009)
- Drake et al, *Nature* 443, 553 (2006)
- Finn,J.M. and Antonsen,T.A., Comm. Plas. Phys. Cont. Fus. 9, 111 (1985)

- Furth H, Killeen J and Rosenbluth MN, *Phys. Fluids* 6, 459 (1963
- Gordovskyy,M. And Browning,P.K. *Ap.J.* 729, 101 (2011)
- Gordovskyy,M. & Browning,P.K. *Sol. Phys* 277, 299 (2012)
- Hahm, T.S. and Kulsrud, R.M., *Phys. Fluids*, 28, 2412 (1985)
- Hannah,I.G. and Fletcher,L. *Sol. Phys.* 236, 59 (2006)
- Hesse,M. et al, *Phys. Plas* 6, 1781 (1999)
- Heyvaerts,J. and Priest,E.R. *Astron. Astrophys.* 137, 63 (1984)
- Hillier.A. et al, *Ap. J.*, 746, 120 (2012)
- Hood,A.W. And Priest *Sol. Phys.* 64, 203 (1979)
- Hood,A.W. et al *Astron. Astrophys* 506, 913 (2009)
- Lin,R.P. *Ap. J.* 595, L69 (2003)
- Linton,M. and Priest,E.R., *Ap. J.* 595, 1259 (2003)
- Longcope,D.W and Cowley,S.C. *Phys Plas. 3, 2885 (1996)*

- Maclean,R. et al *Sol. Phys.* 260, 299 (2009)
- Oz.E. et al *Phys. Plas.* 18, 102107 (2011)
- Pontin,D. *Geophys. Astr. Fluid. Dyn.*99, 77 (2005)
- Pontin,D. *Adv. Space. Res.* 47, 1508 (2011)
- Priest,E.R. and Demoulin,P., *J.G.R.* 100, 23443 (1995)
- Priest,E.R. et al *Ap. J.* 624, 1057 (2005)
- Schrijver,C. and Title,A.,*Sol. Phys.* 207, 223 (2002)
- Stanier, A. et al *Astron. Astrophys. 542, A47* (2012)
- Syrovatskii,S.I. *Sov. Phys. JETP*, 33, 933 (1971)
- Taylor,J.B., *Phys. Rev. Lett*, 33, 1139 (1974)
- Taylor,J.B., *Rev. Mod. Phys.,* 58, 741 (1986)
- Titov,V.S. et al, *Ap. J.* 582, 1172 (2003)
- Vekstein,G. and Jain,R. *Phys. Plasmas.* **5**, 1506 (1998)
- Wood,P. and Neukirch,T. *Sol. Phys.* **226** , 73 (2005)